

Evaluating isolation and contact tracing for control of influenza outbreaks with pandemic potential: a modelling study

Joshua W. Lambert, Adam J. Kucharski

Abstract

Introduction

Outbreaks of severe respiratory infections pose a major public health threat. The COVID-19 pandemic resulted in over 7 million reported deaths (WHO COVID-19 Dashboard), while the 1918 influenza pandemic caused an estimated \sim 50 million deaths (Johnson and Mueller, 2002). Influenza subtypes to which populations have low levels of pre-existing immunity are a particular concern as potential pandemic candidates. This includes influenza A/H5N1 (Ward et al., 2024) and A/H7N9 (Tanner et al., 2015), as well as A/H1N1pdm when it caused a pandemic in 2009 (Fraser et al., 2009). Recent human cases of avian influenza A/H5N1, alongside transmission, further illustrate the ongoing potential for viruses to infect new hosts, creating the potential for further adaption (Antia et al., 2003; Garg et al., 2025; Peacock et al., 2025). It is therefore crucial to understand the effectiveness and feasibility of different intervention strategies in the face of such infections (Fraser et al., 2004; Kucharski, 2024).

Early in a novel outbreak, pharmaceutical options such as treatments and vaccines may not yet be available, leading to reliance on non-pharmaceutical interventions (NPIs) to reduce infection and disease. These interventions include individual-level targeted measures such as isolation and contact tracing, to population-level policies such as venue closures or restrictions on social mixing (Haug et al., 2020; Sharma et al., 2021). The success of such interventions in curtailing transmission before it becomes sustained depends on several factors, including: the type of intervention, timing of introduction, and the intervention's effectiveness (Longini et al., 2005). For highly transmissible pathogens with a short generation times (e.g. pandemic influenza), incidence of new infections can grow quickly, outpacing a response. Moreover, pathogens such as influenza, which have a large proportion of onward transmission prior to symptom onset and have asymptomatic (sub-clinical) cases, are less easily controlled via isolation of symptomatic cases and tracing and quarantining of their contacts (Fraser et al., 2004).

Several pre-COVID-19 studies concluded that influenza viruses cannot be controlled by isolating individuals at symptom onset and tracing their contacts, because the rate at which infected individuals become infectious and transmit is faster than the latency in the process of isolating contacts (Fraser et al., 2004; Klinkenberg et al., 2006). However, with the recent human infections of avian influenza (A/H5N1), mostly among poultry and cattle farmers (Garg et al., 2025) and the longer estimates of incubation period and serial interval from historical A/H5N1 data (Ward et al., 2024) it may be that isolation and contact tracing is able to control influenza subtypes with pandemic potential.

In this study we evaluate the effectiveness of controlling outbreaks that exhibit influenza-like epidemiological characteristics using a mathematical model of isolation and contact tracing. In particular, we investigate the assumption that influenza will inevitably outpace our ability to trace and isolate sufficiently effectively for control, and whether this assumption holds for all pathogen subtypes given emerging estimates of incubation period and serial interval (Ward et al., 2024). Finally, we quantify the speed and effectiveness of isolation for containment under different response delays across epidemic scenarios, and assess the impact of reducing the delay to isolation on outbreak control alongside the use of rapid testing.

Methods

Transmission model

We used a branching process transmission model to assess the potential effectiveness of isolation and contact tracing to control an outbreak of pandemic-potential influenza, implemented in the R package `{ringbp}` (Figure 1) (Hellewell et al., 2025). In the model, each infectious individual generates secondary cases from a negative binomial distribution with a given reproduction number (R) and dispersion parameter (k). Onwards transmission from infectious individuals could be reduced in the following ways: 1) symptomatic individuals isolate effectively, 2) contacts of symptomatic individuals are

traced and isolate if they become symptomatic, 3) contacts of symptomatic individuals are traced and effectively quarantined immediately. Symptomatic individuals that have been traced (i.e. infectees) are isolated at whichever of two events occurs first, either 1) after the onset-to-isolation delay after symptom onset, or 2) when their infector is isolated (if quarantined or symptomatic) or when they become symptomatic if the infector is already isolating.

We include several mechanisms by which isolation and contact tracing can be imperfect at reducing onward disease transmission. The proportion of contacts ascertained by contact tracing can range between 0% (i.e. no contacts are traced) to 100% (i.e. every contact of every symptomatic case is traced). Because the model focuses on onwards transmission prevented, identifying 50% of cases and preventing 100% of their onwards transmission via contact tracing is equivalent to identifying 100% of cases and preventing 50% of their onwards transmission. Subsequent symptomatic cases that have not been contact traced are only isolated after the onset-to-isolation delay post symptom onset. Additionally, we assume infections have an independent probability of being asymptomatic (or paucisymptomatic); these infections were not identified and therefore their contacts were not traced. The advantage of this approach is that it enables estimation of the overall population transmission effect of multiple interventions without requiring each step to be individually specified as a parameter.

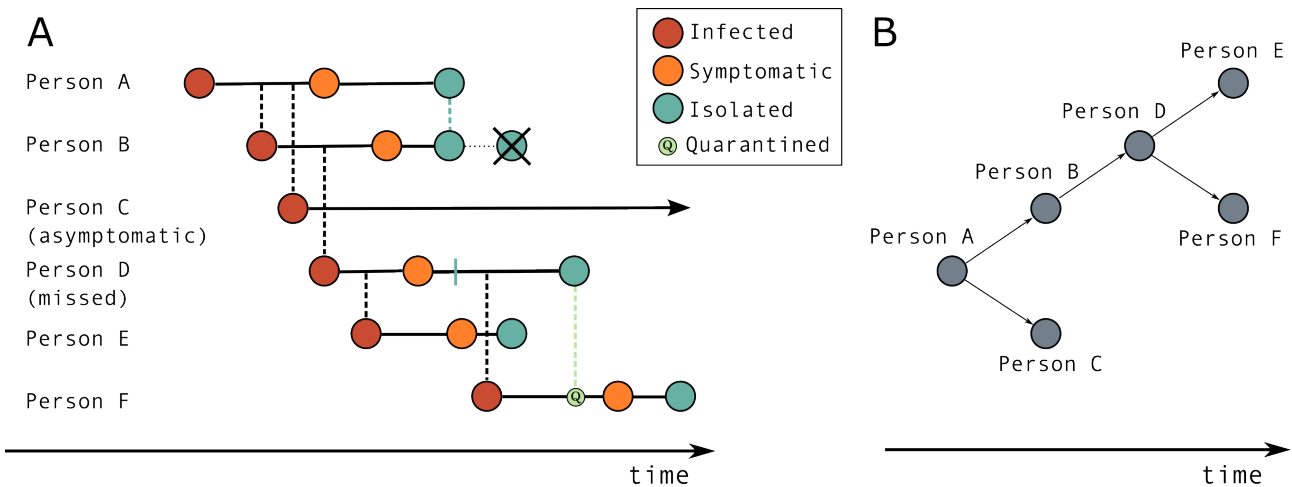


Figure 1: Model schematic of the branching process with isolation, quarantine and contact tracing implemented in the `{ringbp}` R package. (A) The transmission chain from the index case (Person A), infection events are shown by black vertical dashed lines. Individuals can be infected (red circle), become symptomatic (orange circle), and isolated (blue circle). Quarantine is optional in the model, assuming quarantine is active contacts are quarantined when the infector is isolated independent of the contacts symptom status (green circle with Q). The time at which a infectors isolation triggers the isolation of a symptomatic case is shown by the blue vertical dashed line (Person A to Person B). The isolation times that would have been triggered after a delay from symptom onset, but are after isolation was triggered by contact tracing is shown by a blue circle with a cross and connected by a dotted line (Person B). Person C is an asymptomatic individual (asymptomatic cases can infect others). Person D is missed by contact tracing (contacts are traced with a probability ρ , and thus missed at $1 - \rho$). The time Person D would have isolated if ascertained is shown by the vertical blue mark. Assuming quarantine is active, Person F would be isolated before symptom onset at the time of the infector's (Person D) isolation time. If quarantine is not active, then Person F would be isolated after a delay from symptom onset, as they had yet to show symptoms when the infector was isolated. (B) A branching process diagram showing who-infected-whom.

Pathogen epidemiological parameters

In this study we evaluate the feasibility of controlling outbreaks of A/H5N1-, A/H1N1-, and A/H7N9-like infections. The generation time is modelled using the incubation period and the proportion of presymptomatic transmission to simulate a correlated structure between the two delay distributions to generate sensible delays between exposure, symptom onset and onward transmission (Figure 2A) (Hellewell et al., 2020; Linton et al., 2022). We extracted previously estimated incubation periods from the literature for each subtype. Nishiura and Inaba (2011) report the best fitting Weibull shape and scale parameters for H1N1 to be 1.77 and 1.86, respectively (Figure 2B). Cowling et al. (2013) report the incubation period for H5N1 and H7N9, both Weibull distributed. For H5N1 the Weibull distribution has a mean of 3.3 days and standard deviation (SD) of 1.5 days, for H7N9 the Weibull distribution has a mean of 3.1 days and SD 1.4 days (Cowling et al., 2013) (Figure 2B). Comparatively, the incubation period for H1N1 shorter than the other two subtypes (H5N1 and H7N9), which are similar, with H5N1 having a slightly longer median (Figure 2B).

We simulated three presymptomatic transmission scenarios: 1%, 15%, and 30% of transmission occurring prior to symptom onset. We assumed that asymptomatic infections can occur and infect others, but are less common than symptomatic

infectious individuals and that the majority of cases will develop symptoms during their infectious period. We ran scenarios with three different assumed proportion of asymptomatic cases, one with zero asymptomatic illness, another with 10% of cases being asymptomatic and the most extreme scenario where 30% of cases never develop symptoms and thus are not isolated and secondary cases are missed by contact tracing. These proportions of presymptomatic transmission and asymptomatic fraction cover a broad range of possible pandemic influenza possibilities (Figure 3) (Lessler et al., 2009; Xu et al., 2013; Montgomery et al., 2024; Garg et al., 2025).

We considered four reproduction number (R) values when simulating transmission in the community: 1.1, 1.5, 2.5 and 3.5 (Figure 3). These are based on similar values to previously estimated R values for influenza outbreaks (Ferguson et al., 2006), including A/H1N1pdm (Fraser et al., 2009; Lessler et al., 2009), or they represent inflated values of current estimates of A/H5N1 and A/H7N9 subtypes to evaluate the effectiveness of isolation and contact tracing in the event that pathogen evolution enhances the human-to-human transmissibility (e.g. genetic reassortment (Peacock et al., 2025) or mutations in receptor binding preference (Lin et al., 2024)). Once isolated, cases are assumed to not infect anyone ($R_{iso} = 0$). The reproduction number of asymptomatic cases is assumed equal to the community. The dispersion parameter (k) for the negative binomial offspring distributions was fixed at 0.8 for community and asymptomatic cases following evidence that influenza subtypes have moderate transmission heterogeneity (Fraser et al., 2009; He et al., 2020; Ward et al., 2024).

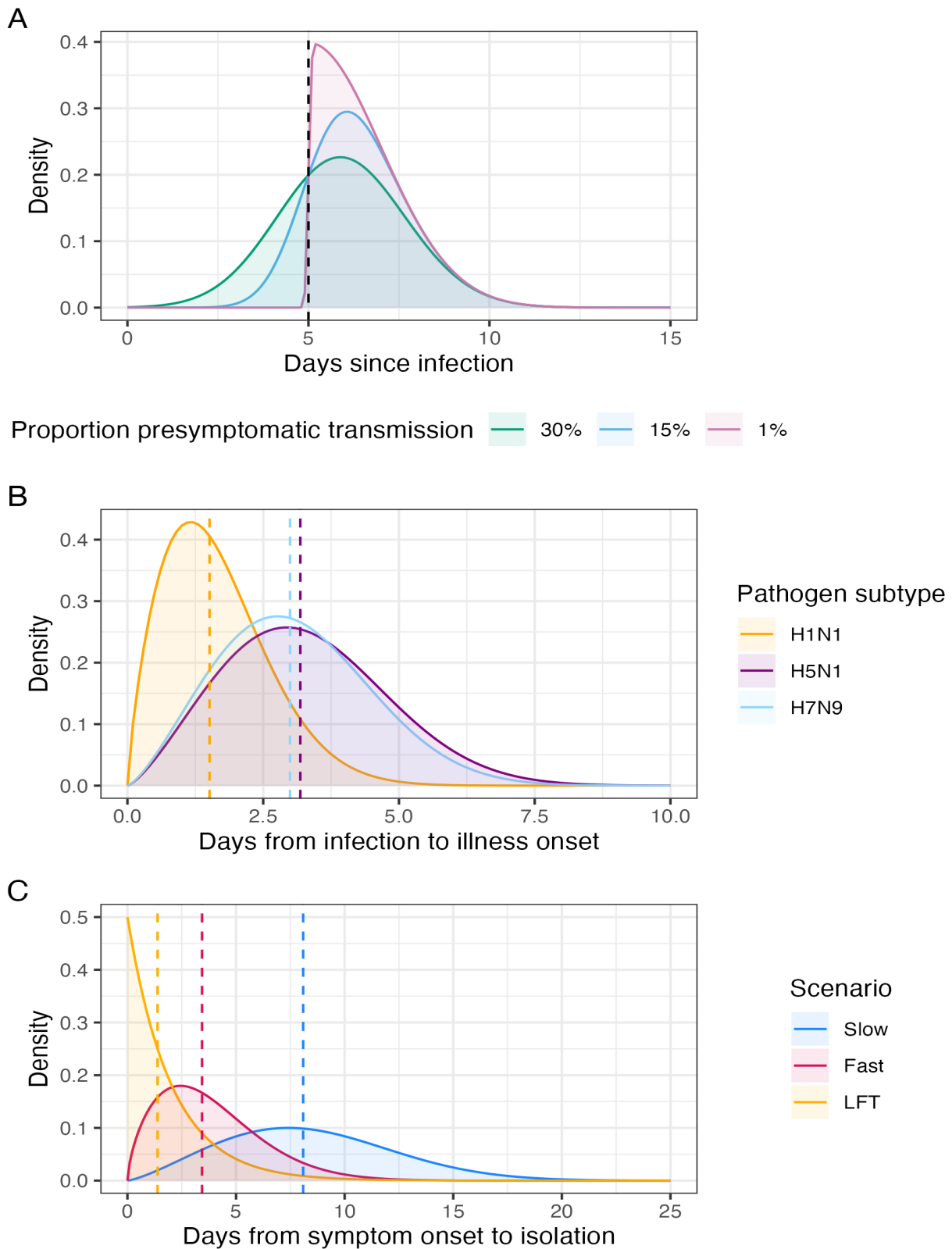


Figure 2: (A) Proportion of presymptomatic transmission determined by the incubation period, here assumed to be 5 days (dashed vertical line), controlled by a skew-normal distribution. Three skew-normal distribution probability density functions are plotted with different skew parameters, 0.73, 1.96, 31.82, which correspond to 30%, 15% and 1% presymptomatic transmission. (B) Incubation period for the influenza subtypes: A/H1N1, A/H5N1 and A/H7N9. The vertical dashed lines are the median incubation period: A/H1N1 is 1.5 days (yellow dashed line), A/H5N1 is 3.2 days (purple dashed line), and A/H7N9 is 3.0 days (blue dashed line). (C) Three assumed onset-to-isolation delays used in the simulation experiment. The *Slow* scenario is based on the onset-to-isolation for the SARS-CoV-2 response in Wuhan, China (Li et al., 2020), the median onset-to-isolation is 8.1 days (blue dashed line). The *Fast* scenario is based on the onset-to-isolation for SARS-CoV-1 response in Hong Kong (Donnelly et al., 2003), the median onset-to-isolation time is 3.4 days (red dashed line). The lateral flow test (LFT) scenario is an assumed distributed for rapid self-administered home testing upon isolation, the median delay from symptom onset to isolation in this scenario is 1.4 days (orange dashed line).

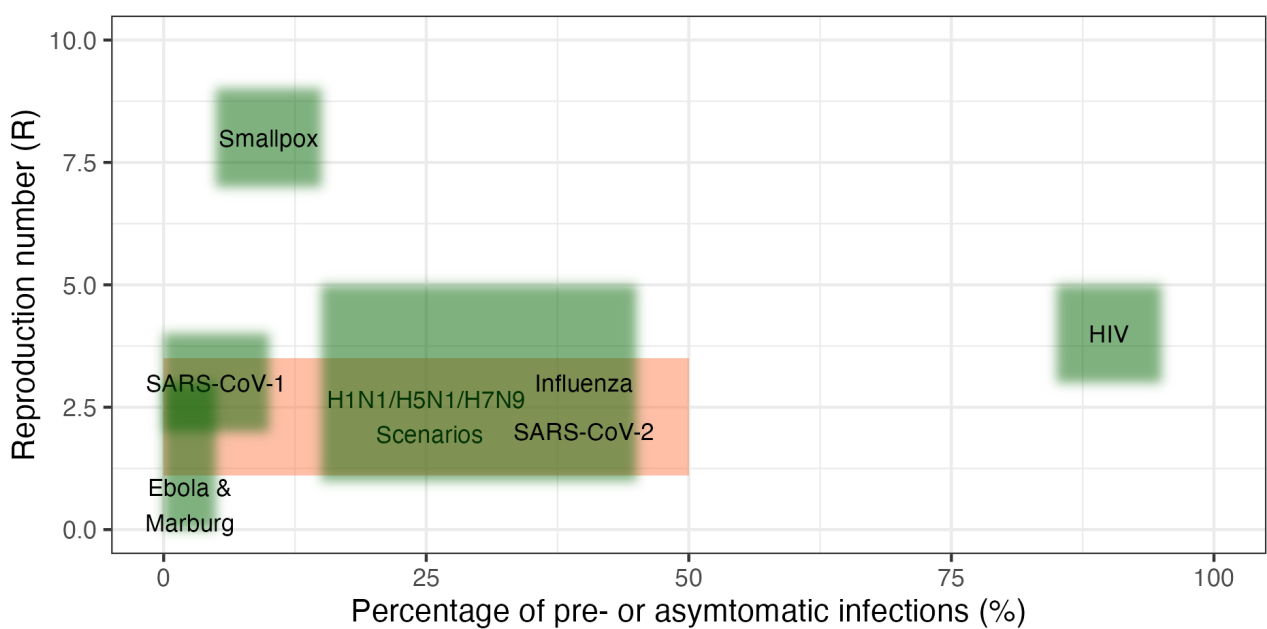


Figure 3: The pathogen characteristics, in terms of transmissibility (R) and proportion of disease transmission that occurs before the onset of symptoms (including cases that are entirely asymptomatic). The figure includes: Influenza, SARS-CoV-1, SARS-CoV-2, Smallpox, Ebola, Marburg, and HIV shown by green shaded areas. The size of the shaded area reflects the differences in pathogen characteristics, both between variants and outbreaks, the blurred edges reflects uncertainty in parameter estimates. The parameter space of transmissibility and pre- and asymptomatic transmission explored in this paper is shown in the orange box.

Scenarios

The onset-to-isolation delay is parameterised under three response scenarios. A fast response, based on the SARS in Hong Kong (Donnelly et al., 2003) and a slower response based on COVID-19 in Wuhan, China (Li et al., 2020) (Figure 2C). Both the fast and slow onset-to-isolation are parameterised as Weibull distributions, the SARS-like distribution has shape (λ) 1.65 and scale (k) 4.29 (mean = 3.83 days, SD = 2.38 days), the COVID-like distribution has shape = 2.31 and scale = 9.48 (mean = 8.40, SD = 3.87 days) (Figure 2C). The third onset-to-isolation scenario is based on a situation where lateral flow rapid tests (LFTs) are provided to all susceptible individuals in the population and these people are freely able to self-test if they are symptomatic. We parameterise this as an exponential distribution, with rate (λ) 0.5, where most individuals will self-test very shortly after they become symptomatic (approximately 40% of cases will self-test within the first day of symptom onset), with a few people waiting a 2 or more days before testing (approximately 3% take longer than one week to take a self-test) (Figure 2C). We assume that LFT sensitivity is 100% accurate so all symptomatic individuals will receive a positive test result.

To assess the feasibility of outbreak containment under different proportions of contacts traced and isolated we varied the proportion of contacts ascertained between 0% (i.e. no contacts traced) and 100% (i.e. all contacts traced) at intervals of 20%. When contact ascertainment is zero, isolation is the only NPI reducing transmission. To test scenarios where an outbreak starts with different number of initial infections, we simulate with either 5, 20 or 40 initial independent cases. This could represent importation of multiple cases in a single event, such as a flight. Lastly, we determine if additionally quarantining contacts, that is isolating contacts once the infector is isolated independent of whether the contact is symptomatic, improves the ability to contain influenza outbreaks.

Defining outbreak control

We define outbreak control as no new cases after 12 weeks from the start of an outbreak. The rationale for this criteria is that some outbreaks that do not take off and become sustained may still have cases for the first few weeks of an outbreak, therefore the window for control needs to be enough time after the seeding of an outbreak to be sure it is contained (Hellewell et al., 2020). Due to the exponential dynamics of outbreaks and no depletion of susceptibles in our model we implement a maximum number of cases in each simulation. When this cumulative case limit is reached, it is judged to be a sustained epidemic, not controllable within 12 weeks. We set this limit to 5,000 cases.

Results

The reproduction number, contact tracing ascertainment and speed of isolation all affect the ability to control a pandemic potential influenza outbreak (Figure 4). Isolation alone can control over 50% of epidemics with an R of 1.1 with a slow onset-to-isolation response (median 8.1 days); while a fast (median 3.4 days) or LFT (median 1.4 days) response almost always controls $R = 1.1$ outbreaks (Figure 4). When $R = 1.5$, >75% of contacts need to be traced to control at least 75% of outbreaks for a slow onset-to-isolation, whereas only 40% of contacts require tracing for at least 75% controlled under a fast isolation delay (Figure 4A,B). The isolation upon rapid LFT self-testing controls epidemics with $R \leq 1.5$ without tracing contacts (Figure 4C). High transmissibility scenarios ($R \geq 2.5$) require comprehensive contact tracing to contain at least 50% of simulated outbreaks (~100% for a slow response and ~80-100% for a fast response). Isolation and tracing 80% of contacts using LFTs to trigger isolation controls over 80% of simulated outbreaks for all subtype and transmissibility scenarios (Figure 4C).

There is some variability in the effectiveness of isolation and contact tracing for outbreak control between influenza subtypes. A/H1N1, because of its shorter incubation period and thus faster tempo of transmission, has a lower proportion of outbreaks controlled, most noticeably for $R \geq 1.5$ (Figure 4). There is not a strong pattern for the variance in outbreak control between influenza subtypes across scenarios; the few scenarios with higher variance between subtypes are at high percentages of contacts traced ($\geq 60\%$) and for high transmissibility scenarios (Figure S1).

Increased presymptomatic transmission and asymptomatic cases decreases epidemic containment (Figure S2 and S3). When 30% of transmission occurs before symptom onset, in high transmissibility scenarios ($R \geq 2.5$) more than half of outbreaks become sustained epidemics for all onset-to-isolation delays (Figure S2). When only 1% of transmission is presymptomatic and contact tracing ascertains all contacts, outbreaks with $R = 3.5$ are contained in >75% of outbreaks with LFT testing, and in ~25% of outbreaks with a fast isolation response (Figure S2). When all cases develop symptoms, isolation and contact tracing all contacts can control all outbreak scenarios, with the sole exception being A/H1N1 with $R = 3.5$ and a slow onset-to-isolation (Figure S3). When 10% of cases are asymptomatic the ability to contain highly transmissible influenza ($R \geq 2.5$) dramatically decreases, and decreases further when 30% of cases are asymptomatic or paucisymptomatic, even with comprehensive contact tracing and isolation upon LFT self-testing, less than a quarter of outbreaks are contained (Figure S3).

The more cases that initially seed an outbreak with $R \geq 1$, the less chance that it will stochastically go extinct and we find that the higher the number of initial influenza cases reduces the efficacy of control-by-isolation (Figure 5). Isolation alone can control outbreaks with $R = 1.1$ even when seeded with 40 initial cases (Figure 5). When $R \geq 1.5$ increasing the number of initial cases makes epidemics less controllable for all influenza subtypes. For high transmissibility ($R \geq 2.5$) scenarios that are seeded with at least 20 cases, close to 100% of contacts need to be traced and isolated upon symptom onset to control the majority of outbreaks, assuming a fast onset-to-isolation response (3.4 days on average) (Figure 5).

In the acute phase of outbreaks there can be thousands of weekly cases, especially for high transmissibility scenarios ($R \geq 2.5$) (Figure S5). Specifically for controlled outbreaks, the cumulative number of cases is consistently below 500 cases across influenza subtypes (Figure S4). Thus when an outbreak is controlled with isolation alone or in combination with contact tracing it is done so without incurring a high initial prevalence.

The control of influenza outbreaks with a $R > 1$ require interventions to bring R below 1 for transmission to eventually cease. Isolation of symptomatic cases alone reduces R (Figure 6). When the delay between symptom onset and isolation is around 8 days (i.e. slow response), the reduction in R can be minimal, whereas if isolation is rapid after symptom onset, around 1.5 days (i.e. LFT self-testing response), isolation without contact tracing or quarantine brings R_t below 1 when $R_0 < 3$ (Figure 6). Contact tracing can further suppress transmission, with 100% contact ascertainment bringing an outbreak under control ($R < 1$) for all influenza subtypes and isolation responses for $R_0 < 2.5$ (Figure 6). Quarantine has a negligible impact on the reducing disease transmission, with a slightly greater reduction in transmission when there is a higher proportion of presymptomatic transmission (Figure 6 and S6). The effectiveness of tracing and isolating contacts is reduced when more cases transmit before symptomatic or are asymptomatic (Figure 6 and S6).

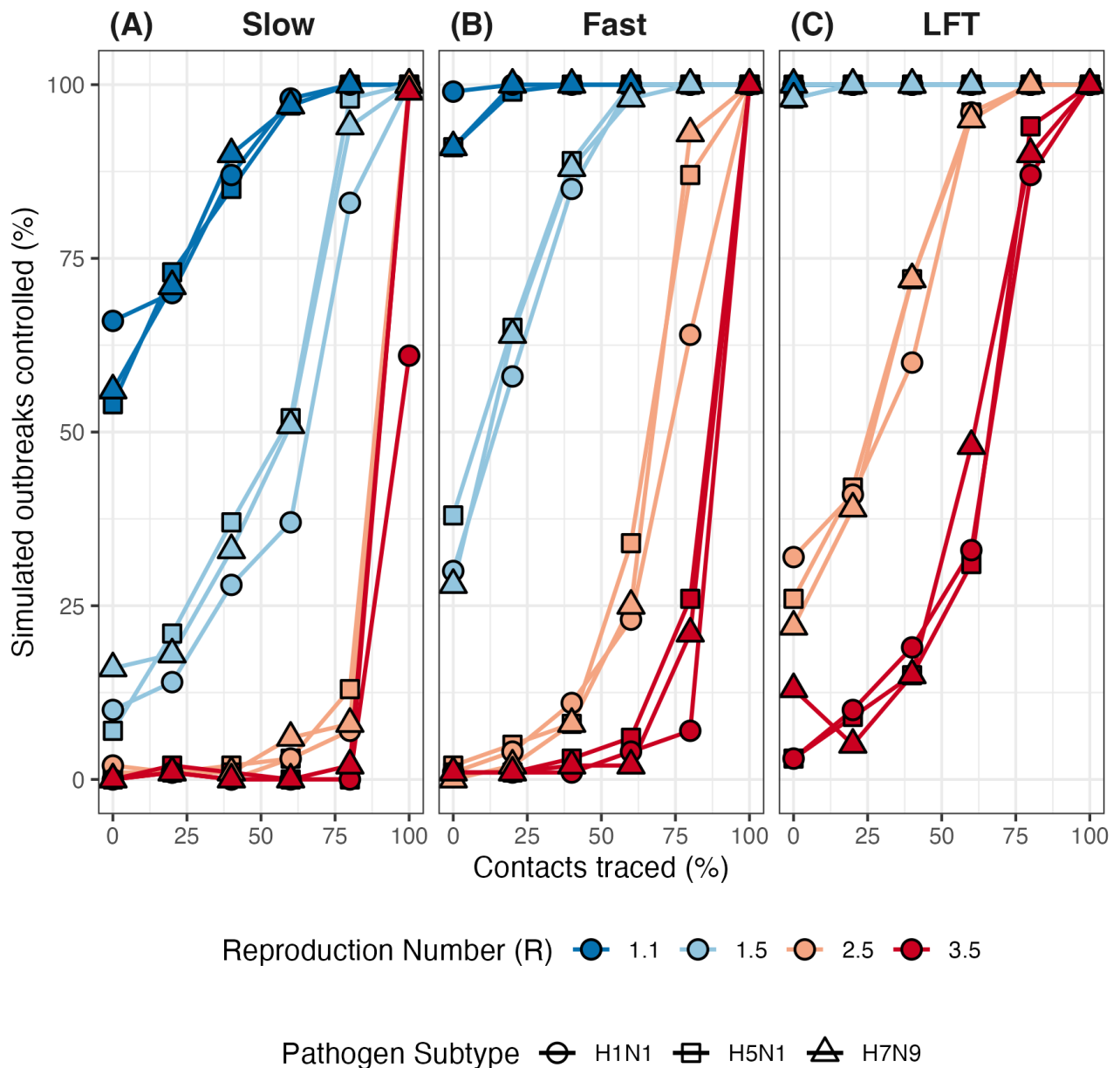


Figure 4: The percentage of outbreaks controlled across values of isolation and contact tracing effectiveness, for outbreaks with an assumed reproduction number (R) of either 1.1 or 1.5. This is for a baselines scenario where the number of initial cases is 10, the proportion of presymptomatic transmission is 15%, all cases are assumed symptomatic, and the onset-to-isolation delay is assumed to be SARS-like.

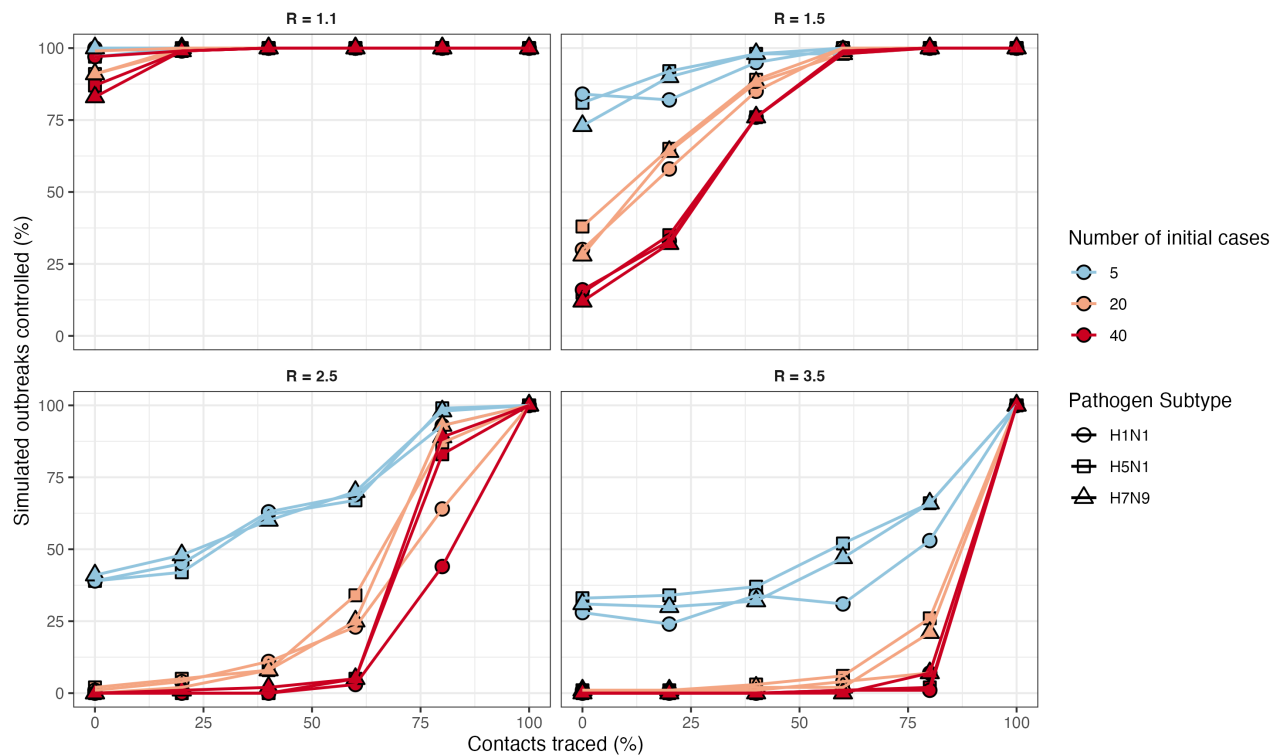


Figure 5: The percentage of outbreaks controlled across values of isolation and contact tracing effectiveness, for outbreaks with an initial number of seeding infections assumed to be either 5 or 10. This is for a baselines scenario where the reproduction number is 1.5, the proportion of presymptomatic transmission is 15%, all cases are assumed symptomatic, and the onset-to-isolation delay is assumed to be SARS-like.

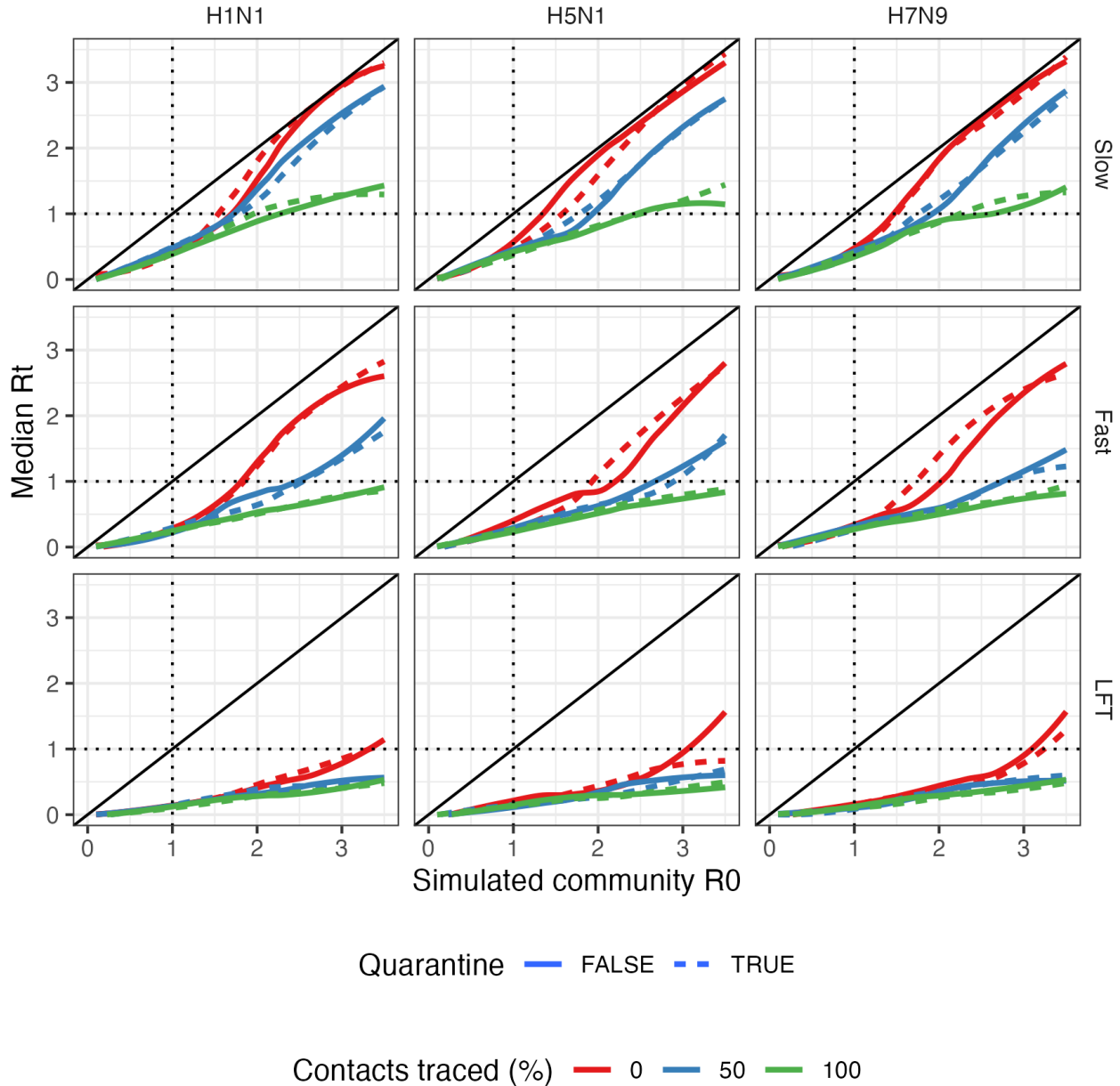


Figure 6: The median effective reproduction number (R_t) across simulation replicates calculated from simulated outbreak data under various influenza subtype and intervention scenarios against the basic reproduction number (R_0) for the general community used to simulate the outbreaks. The R_0 value for isolated cases is zero. The diagonal line shows an equal value for R_t and community R_0 . The dotted lines are where the values of R_t (horizontal) or community R_0 (vertical) equal unity. Values of R_t below the diagonal indicate a reduction in transmission from NPIs compared to uncontrolled community transmission. Isolation of symptomatic cases is active for all scenarios, contact tracing ascertainment is plotted for 0% (no contact tracing), 50% and 100% (all symptomatic contacts of symptomatic cases traced), we run each scenario with quarantine of contacts active (dashed line) and inactive (solid line). This is for a baseline scenario where the proportion of presymptomatic transmission is 1% and the proportion of asymptomatic cases is 0%.

Discussion

Influenza remains a high risk pathogen with pandemic potential as shown by the history of influenza pandemics throughout the 20th century (Saunders-Hastings and Krewski, 2016). The recent spread of A/H5N1 avian influenza in cattle and poultry farms, primarily in the US, creates a greater spillover risk and adaptations to enhance mammal-to-mammal transmission (Lin et al., 2024; Garg et al., 2025; Peacock et al., 2025). In this study we use a mathematical model to assess the feasibility and effectiveness of isolation and contact tracing for avian and non-avian influenza subtypes to determine whether these should be considered effective NPIs in the event that sustained human-to-human transmission is detected.

We find that the percentage of contacts that need to be successfully traced to control an outbreak depends on the reproduction number of the pathogen, and the speed at which a public health system can respond by testing and communicating with those infected and contacts of infectious persons. If the delay between symptom onset and isolation is at least one week, then isolation and comprehensive contact tracing are required to be confident a moderate to highly transmissible ($R \geq 1.5$) influenza can be controlled. By reducing the delay between symptom onset and isolation to around three days, influenza pathogens that are marginally supercritical ($R = 1.1$) become subcritical ($R < 1$) and contained by isolation alone, and more transmissible scenarios can be controlled with good contact tracing coverage. In addition to two empirically-based onset-to-isolation delays, by testing a rapid isolation scenario where LFTs that do not require a test being sent to a laboratory, as would be the case for polymerase chain reaction (PCR) testing, the benefit to containment probability, and the opportunity to control highly transmissible ($R \geq 2.5$) respiratory diseases with isolation and contact tracing. Therefore, the dogma that symptom-based isolation and contact tracing are not effective for influenza is shown not to hold for optimal testing and isolation scenarios, even if some cases are missed due to being asymptomatic and some transmission occurs prior to symptom onset. If making LFTs widely accessible is economical relative to the cost of mass contact tracing, a low to moderate transmissibility influenza pandemic response should focus on reducing the onset-to-isolation response. Whether the interventions proposed here are cost-effective remains a question for further investigation.

The transmission model highlights the bimodal nature of the final size of outbreaks, where NPI-controlled epidemics typically range from tens to hundreds of total cases, in contrast, uncontrolled outbreaks can produce thousands of new cases each week. The severity of avian influenza subtypes is uncertain, historical estimates are $\sim 30\% - 55\%$ (Tanner et al., 2015), but recent human infections have lower morbidity and mortality (Garg et al., 2025; Krammer et al., 2025). Consequently, the difference in disease burden between containing an outbreak while still small compared to allowing thousands of cases will be substantial. Even if updated severity estimates are significantly lower, widespread infections could still result in a devastating outcome.

It is possible that a sentinel surveillance system or community testing to detect new cases of pandemic potential influenza (e.g. A/H5N1 or A/H7N9), could miss the primary case(s), whether originating from zoonotic spillover or importation. We show that more cases before an NPI is activated hinders the ability to effectively contain the outbreak. The magnitude of this impact is moderated more by transmissibility than influenza subtype for the three variants we considered. If interventions are activated when case prevalence exceeds 50 cases, then even rapidly isolating over 60% of people with 2 days of becoming symptomatic will require near-perfect contact tracing coverage. For comparison, on the date of the first fatality in the UK from COVID-19 there were already over 100 confirmed cases and probable sustained widespread community transmission. A subcritical influenza outbreak could cause transient epidemics, during which, adaptation to enhance human-to-human transmission can cause a critical transition to supercritical transition, at which point more importations exponentially decreases containment without interventions (Whittle, 1955; Farrington and Grant, 1999; Antia et al., 2003; Lloyd-Smith et al., 2005). This study does not model this transition, instead we assume supercritical human-to-human transmission potential for A/H5N1 and A/H7N9 to evaluate NPIs because current estimates for pathogen epidemiology ($R < 1$) do not require interventions for containment. Cases detected with routine surveillance without a known animal source may indicate sustained human-to-human transmission and could be a trigger to commence isolation and contact tracing while the number of initial cases is presumed small.

The strength of our approach is based on the simple parameterisation of the individual-based model to capture the infectiousness, disease progression and onward transmission incorporating individual-level heterogeneity. Sampling the generation time using the incubation period and proportion of presymptomatic infections (using a skew-normal distribution) enables simulating transmission dynamics for novel pathogens and early in outbreaks when the incubation period is estimated but the generation time is unknown or estimated with more uncertainty, and the serial interval would introduce bias if used instead (Britton and Scalia Tomba, 2019; Lehtinen et al., 2021).

The model and simulation experiment has several limitations. We assumed that the LFT rapid tests are accurate and do not provide false negatives, in reality these type II errors will result in a smaller reduction in transmission (Peto et al., 2021). Secondly, the isolation of infectious individuals is assumed to prevent all onward transmission. This may be overly conservative if for example individuals isolate at home while living with others, who may become infected and continue to spread the disease until they become symptomatic and isolate. We find that quarantine has a negligible reduction – and

counter intuitively in some cases a small increase – in reproduction number. This is likely due to the model implementation of quarantine, whereby ..., and should not be concluded that quarantine is ineffective for respiratory pathogens. Lastly, the transmission model does not take into account network or age structure which has been shown to influence the effectiveness of isolation and contact tracing (Juul and Strogatz, 2023).

We assessed the benefit of contact tracing across a range of possible contact ascertainment levels. In doing so we model up to 5,000 cases before terminating a simulated outbreak as uncontained, but before reaching the case limit we assume that there is no capacity limit on contact tracing. This is an optimistic assumption; in reality surveillance systems can be patchy and have finite capacity, exacerbated in resource-limited settings (Dhillon and Srikrishna, 2018). The scenarios where a low percentage of contacts were traced may be more representative for these situations. The finding that weekly case incidence can reach thousands of new cases within the acute phase of an influenza outbreak highlights how the exponential dynamics of outbreaks, even in the presence of NPIs, can overburden surveillance systems with the volume of testing and isolation required. Aside from public health surveillance capacity, we also ignore potential socio-political factors that may prevent contacting infected individuals or contacts of infected individuals (Dhillon and Srikrishna, 2018). In this study we assume that contacts are known, avoiding the need to define what constitutes a contact. In reality the threshold for duration and distance of a contact for a directly transmitted respiratory disease will influence the ascertainment and volume of contact tracing required by balancing the error rates of contacts that result in infections (Keeling et al., 2020).

The experience of contact tracing from the COVID-19 pandemic has shown that isolating and quarantining contacts can be expedited with the use of digital tracing. As opposed to symptom-based testing and isolating, a contact can be determined by proximity and duration between mobile devices, and if someone tests positive it can immediately notify all recent contacts (Ferretti et al., 2020). This approach would be complimentary to the LFT scenario in this study where available rapid tests could be used when notified of an infectious contact (assuming the time between exposure and testing is longer than the detectable latent period). Decentralising contact tracing to devices most people carry around at all times (e.g. smartphones) would also ease capacity limitations of a centralised contact tracing unit. The optimistic scenarios of traditional testing, tracing and isolating included could in theory be improved and epidemic prevention enhanced by integrating digital technology.

Enacting isolation and contact tracing and other NPIs is expected with the emergence of a novel pathogen due to widespread susceptibility and no pharmaceutical interventions. However, influenza has multiple circulating seasonal subtypes and past pandemics, resulting in a complex mosaic of population immunity for different influenza subtypes, with possible immunological imprinting (Gostic et al., 2016). There is also seasonal vaccination availability in many high- and middle income countries (Goldin et al., 2024), stockpiles of vaccines for avian influenza, as well as licensed effective antivirals (Krammer et al., 2025). We show that asymptomatic influenza infections will detrimentally influence containment with symptom-based isolation and contact tracing. If an epidemic is highly asymptomatic ($> 25\%$ cases), countries with a stockpile of influenza antivirals, could deploy those prophylactically in response (Hayden, 2001). For example, the UK which stockpiles antivirals for $\sim 50\%$ of the population (Wri). Pandemic response could deploy pharmaceutical and non-pharmaceutical interventions in combination to prevent disease burden by suppressing transmission and severity. The stockpile of vaccines for A/H5N1 that shows cross-reactivity with current 2.3.4.4b strain are another line of defence (Khurana et al., 2024). The speed of isolating contacts compared to vaccinating them in the context of a fast generation time and proportion of presymptomatic transmission, renders a ring vaccination less effective (Kucharski et al., 2016; Whittaker et al., 2024). Overall, the response to an influenza pandemic from an avian or swine subtype would be more multifaceted than the baseline containment results from our model.

Our study shows that isolation and contact tracing are effective NPIs that should be considered when evaluating a robust outbreak response to pandemic potential influenza. If responding to a pathogen where human-to-human transmission is sustained ($R \leq 1.5$) isolation of symptomatic cases alone will bring the reproduction number below one, and comprehensive tracing and isolation of contacts with a short delay to isolation can control outbreaks with $R \leq 3.5$. Whether the next public health emergency is from avian (A/H5N1 and A/H7N9) or swine (A/H1N1) influenza, the response should be broadly similar. If in the acute phase of the outbreak clinical and epidemiological investigation indicate presymptomatic transmission or asymptomatic infections (Liu et al., 2020), or that multiple imported cases have seeded human-to-human transmission chains (Russell et al., 2021), then increasing contact tracing ascertainment and reducing the onset-to-isolation delay will improve chances of containment. Our results broadly cover to novel emerging pathogens that lack pharmaceutical interventions; extending results to other pandemic pathogen candidates depends on the similarity of their epidemiological characteristics.

References

Written questions and answers - Written questions, answers and statements - UK Parliament. <https://questions-statements.parliament.uk/written-questions/detail/2021-10-15/57051>.

Tjandra Y. Aditama, Gina Samaan, Rita Kusriastuti, Ondri Dwi Sampurno, Wilfried Purba, null Misriyah, Hari Santoso, Arie

Bratasena, Anas Maruf, Elvieda Sariwati, Vivi Setiawaty, Kathryn Glass, Kamalini Lokuge, Paul M. Kelly, and I. Nyoman Kandun. Avian influenza H5N1 transmission in households, Indonesia. *PLoS One*, 7(1):e29971, 2012. ISSN 1932-6203. doi: 10.1371/journal.pone.0029971.

Rustom Antia, Roland R. Regoes, Jacob C. Koella, and Carl T. Bergstrom. The role of evolution in the emergence of infectious diseases. *Nature*, 426(6967):658–661, December 2003. ISSN 0028-0836, 1476-4687. doi: 10.1038/nature02104.

A. Azzalini. A Class of Distributions Which Includes the Normal Ones. *Scandinavian Journal of Statistics*, 12(2):171–178, 1985.

Tom Britton and Gianpaolo Scalia Tomba. Estimation in emerging epidemics: Biases and remedies. *Journal of The Royal Society Interface*, 16(150):20180670, January 2019. ISSN 1742-5689, 1742-5662. doi: 10.1098/rsif.2018.0670.

Benjamin J. Cowling, Lianmei Jin, Eric H. Y. Lau, Qiaohong Liao, Peng Wu, Hui Jiang, Tim K. Tsang, Jiandong Zheng, Vicky J. Fang, Zhaorui Chang, Michael Y. Ni, Qian Zhang, Dennis K. M. Ip, Jianxing Yu, Yu Li, Liping Wang, Wenxiao Tu, Ling Meng, Joseph T. Wu, Huiming Luo, Qun Li, Yuelong Shu, Zhongjie Li, Zijian Feng, Weizhong Yang, Yu Wang, Gabriel M. Leung, and Hongjie Yu. Comparative epidemiology of human infections with avian influenza A H7N9 and H5N1 viruses in China: A population-based study of laboratory-confirmed cases. *Lancet (London, England)*, 382(9887):129–137, July 2013. ISSN 1474-547X. doi: 10.1016/S0140-6736(13)61171-X.

Ranu S Dhillon and Devabhaktuni Srikrishna. When is contact tracing not enough to stop an outbreak? *The Lancet Infectious Diseases*, 18(12):1302–1304, December 2018. ISSN 14733099. doi: 10.1016/S1473-3099(18)30656-X.

Christl A Donnelly, Azra C Ghani, Gabriel M Leung, Anthony J Hedley, Christophe Fraser, Steven Riley, Laith J Abu-Raddad, Lai-Ming Ho, Thuan-Quoc Thach, Patsy Chau, King-Pan Chan, Tai-Hing Lam, Lai-Yin Tse, Thomas Tsang, Shao-Haei Liu, James Hb Kong, Edith Mc Lau, Neil M Ferguson, and Roy M Anderson. Epidemiological determinants of spread of causal agent of severe acute respiratory syndrome in Hong Kong. *The Lancet*, 361(9371):1761–1766, May 2003. ISSN 01406736. doi: 10.1016/S0140-6736(03)13410-1.

C. P. Farrington and A. D. Grant. The distribution of time to extinction in subcritical branching processes: Applications to outbreaks of infectious disease. *Journal of Applied Probability*, 36(3):771–779, September 1999. ISSN 0021-9002, 1475-6072. doi: 10.1239/jap/1032374633.

Neil M. Ferguson, Derek A. T. Cummings, Christophe Fraser, James C. Cajka, Philip C. Cooley, and Donald S. Burke. Strategies for mitigating an influenza pandemic. *Nature*, 442(7101):448–452, July 2006. ISSN 1476-4687. doi: 10.1038/nature04795.

Luca Ferretti, Chris Wymant, Michelle Kendall, Lele Zhao, Anel Nurtay, Lucie Abeler-Dörner, Michael Parker, David Bonsall, and Christophe Fraser. Quantifying SARS-CoV-2 transmission suggests epidemic control with digital contact tracing. *Science*, 368(6491), May 2020. ISSN 0036-8075, 1095-9203. doi: 10.1126/science.abb6936.

Christophe Fraser, Steven Riley, Roy M. Anderson, and Neil M. Ferguson. Factors that make an infectious disease outbreak controllable. *Proceedings of the National Academy of Sciences of the United States of America*, 101(16):6146–6151, April 2004. ISSN 0027-8424. doi: 10.1073/pnas.0307506101.

Christophe Fraser, Christl A. Donnelly, Simon Cauchemez, William P. Hanage, Maria D. Van Kerkhove, T. Déirdre Hollingsworth, Jamie Griffin, Rebecca F. Baggaley, Helen E. Jenkins, Emily J. Lyons, Thibaut Jombart, Wes R. Hinsley, Nicholas C. Grassly, Francois Balloux, Azra C. Ghani, Neil M. Ferguson, Andrew Rambaut, Oliver G. Pybus, Hugo Lopez-Gatell, Celia M. Alpuche-Aranda, Ietza Bojorquez Chapela, Ethel Palacios Zavala, Dulce Ma Espejo Guevara, Francesco Checchi, Erika Garcia, Stephane Hugonnet, Cathy Roth, and WHO Rapid Pandemic Assessment Collaboration. Pandemic potential of a strain of influenza A (H1N1): Early findings. *Science (New York, N.Y.)*, 324(5934):1557–1561, June 2009. ISSN 1095-9203. doi: 10.1126/science.1176062.

Shikha Garg, Katie Reinhart, Alexia Couture, Krista Kniss, C. Todd Davis, Marie K. Kirby, Erin L. Murray, Sophie Zhu, Vit Kraushaar, Debra A. Wadford, Cara Drehoff, Allison Kohnen, Mackenzie Owen, Jennifer Morse, Seth Eckel, Jessica Goswitz, George Turabelidze, Steve Krager, Anna Unutzer, Emilio R. Gonzales, Cherissa Abdul Hamid, Sascha Ellington, Alexandra M. Mellis, Alicia Budd, John R. Barnes, Matthew Biggerstaff, Michael A. Jhung, Malia Richmond-Crum, Erin Burns, Tom T. Shimabukuro, Timothy M. Uyeki, Vivien G. Dugan, Carrie Reed, and Sonja J. Olsen. Highly Pathogenic Avian Influenza A(H5N1) Virus Infections in Humans. *New England Journal of Medicine*, 392(9):843–854, February 2025. ISSN 0028-4793, 1533-4406. doi: 10.1056/NEJMoa2414610.

Shoshanna Goldin, Donald Brooks, Pernille Jorgensen, Pushpa Wijesinghe, Heeyoun Cho, Rania Attia, Reena Doshi, Francisco Nogareda, Belinda Herring, Laure Dumolard, Randie Gibson, Christopher Chadwick, Shalini Desai, Alba Vilajeliu, Ann Lindstrand, Stefano Tempia, Joshua Mott, and Sarah Hess. Seasonal influenza vaccination: A global review of national policies in 194 WHO member states in 2022. *Vaccine*, 42(26):126274, December 2024. ISSN 0264410X. doi: 10.1016/j.vaccine.2024.126274.

Katelyn M. Gostic, Monique Ambrose, Michael Worobey, and James O. Lloyd-Smith. Potent protection against H5N1 and H7N9 influenza via childhood hemagglutinin imprinting. *Science*, 354(6313):722–726, November 2016. ISSN 0036-8075, 1095-9203. doi: 10.1126/science.aag1322.

Nina Haug, Lukas Geyrhofer, Alessandro Londei, Elma Dervic, Amélie Desvars-Larrive, Vittorio Loreto, Beate Pinior, Stefan Thurner, and Peter Klimek. Ranking the effectiveness of worldwide COVID-19 government interventions. *Nature Human Behaviour*, 4(12):1303–1312, November 2020. ISSN 2397-3374. doi: 10.1038/s41562-020-01009-0.

F. G. Hayden. Perspectives on antiviral use during pandemic influenza. *Philosophical Transactions of the Royal Society of London. Series B, Biological Sciences*, 356(1416):1877–1884, December 2001. ISSN 0962-8436. doi: 10.1098/rstb.2001.1007.

Daihai He, Shi Zhao, Yingke Li, Peihua Cao, Daozhou Gao, Yijun Lou, and Lin Yang. Comparing COVID-19 and the 1918–19 influenza pandemics in the United Kingdom. *International Journal of Infectious Diseases*, 98:67–70, September 2020. ISSN 12019712. doi: 10.1016/j.ijid.2020.06.075.

Joel Hellewell, Sam Abbott, Amy Gimma, Nikos I Bosse, Christopher I Jarvis, Timothy W Russell, James D Munday, Adam J Kucharski, W John Edmunds, Sebastian Funk, Rosalind M Eggo, Fiona Sun, Stefan Flasche, Billy J Quilty, Nicholas Davies, Yang Liu, Samuel Clifford, Petra Klepac, Mark Jit, Charlie Diamond, Hamish Gibbs, and Kevin Van Zandvoort. Feasibility of controlling COVID-19 outbreaks by isolation of cases and contacts. *The Lancet Global Health*, 8(4):e488–e496, April 2020. ISSN 2214109X. doi: 10.1016/S2214-109X(20)30074-7.

Joel Hellewell, Sam Abbott, Amy Gimma, Tim Lucas, Sebastian Funk, and Adam Kucharski. *Ringbp: Simulate and Evaluate Contact Tracing Scenarios*, 2025.

Niall P. A. S. Johnson and Juergen Mueller. Updating the Accounts: Global Mortality of the 1918–1920 "Spanish" Influenza Pandemic. *Bulletin of the History of Medicine*, 76(1):105–115, March 2002. ISSN 1086-3176. doi: 10.1353/bhm.2002.0022.

Matt J Keeling, T Deirdre Hollingsworth, and Jonathan M Read. Efficacy of contact tracing for the containment of the 2019 novel coronavirus (COVID-19). *Journal of Epidemiology and Community Health*, 74(10):861–866, October 2020. ISSN 0143-005X, 1470-2738. doi: 10.1136/jech-2020-214051.

Surender Khurana, Lisa R. King, Jody Manischewitz, Olivia Posadas, Ashish K. Mishra, Dongxiao Liu, John H. Beigel, Rino Rappuoli, John S. Tsang, and Hana Golding. Licensed H5N1 vaccines generate cross-neutralizing antibodies against highly pathogenic H5N1 clade 2.3.4.4b influenza virus. *Nature Medicine*, 30(10):2771–2776, October 2024. ISSN 1078-8956, 1546-170X. doi: 10.1038/s41591-024-03189-y.

Don Klinkenberg, Christophe Fraser, and Hans Heesterbeek. The Effectiveness of Contact Tracing in Emerging Epidemics. *PLoS ONE*, 1(1):e12, December 2006. ISSN 1932-6203. doi: 10.1371/journal.pone.0000012.

Florian Krammer, Enikö Hermann, and Angela L. Rasmussen. Highly pathogenic avian influenza H5N1: History, current situation, and outlook. *Journal of Virology*, 99(4):e02209–24, April 2025. ISSN 0022-538X, 1098-5514. doi: 10.1128/jvi.02209-24.

Adam J. Kucharski. Controlling minor outbreaks is necessary to prepare for major pandemics. *PLOS Biology*, 22(12):e3002945, December 2024. ISSN 1545-7885. doi: 10.1371/journal.pbio.3002945.

Adam J. Kucharski, Rosalind M. Eggo, Conall H. Watson, Anton Camacho, Sebastian Funk, and W. John Edmunds. Effectiveness of Ring Vaccination as Control Strategy for Ebola Virus Disease. *Emerging Infectious Diseases*, 22(1):105–108, January 2016. ISSN 1080-6040, 1080-6059. doi: 10.3201/eid2201.151410.

Adam J Kucharski, Timothy W Russell, Charlie Diamond, Yang Liu, John Edmunds, Sebastian Funk, Rosalind M Eggo, Fiona Sun, Mark Jit, James D Munday, Nicholas Davies, Amy Gimma, Kevin Van Zandvoort, Hamish Gibbs, Joel Hellewell, Christopher I Jarvis, Sam Clifford, Billy J Quilty, Nikos I Bosse, Sam Abbott, Petra Klepac, and Stefan Flasche. Early dynamics of transmission and control of COVID-19: A mathematical modelling study. *The Lancet Infectious Diseases*, 20(5):553–558, May 2020. ISSN 14733099. doi: 10.1016/S1473-3099(20)30144-4.

Sonja Lehtinen, Peter Ashcroft, and Sebastian Bonhoeffer. On the relationship between serial interval, infectiousness profile and generation time. *Journal of The Royal Society Interface*, 18(174):20200756, January 2021. ISSN 1742-5689, 1742-5662. doi: 10.1098/rsif.2020.0756.

Justin Lessler, Nicholas G. Reich, Derek A. T. Cummings, New York City Department of Health and Mental Hygiene Swine Influenza Investigation Team, H. P. Nair, H. T. Jordan, and N. Thompson. Outbreak of 2009 pandemic influenza A (H1N1) at a New York City school. *The New England Journal of Medicine*, 361(27):2628–2636, December 2009. ISSN 1533-4406. doi: 10.1056/NEJMoa0906089.

Chengjun Li and Hualan Chen. H7N9 Influenza Virus in China. *Cold Spring Harbor Perspectives in Medicine*, 11(8):a038349, August 2021. ISSN 2157-1422. doi: 10.1101/cshperspect.a038349.

Qun Li, Lei Zhou, Minghao Zhou, Zhiping Chen, Furong Li, Huanyu Wu, Nijuan Xiang, Enfu Chen, Fenyang Tang, Dayan Wang, Ling Meng, Zhiheng Hong, Wenxiao Tu, Yang Cao, Leilei Li, Fan Ding, Bo Liu, Mei Wang, Rongheng Xie, Rongbao Gao, Xiaodan Li, Tian Bai, Shumei Zou, Jun He, Jiayu Hu, Yangting Xu, Chengliang Chai, Shiwen Wang, Yongjun Gao, Lianmei Jin, Yanping Zhang, Huiming Luo, Hongjie Yu, Jianfeng He, Qi Li, Xianjun Wang, Lidong Gao, Xinghuo Pang, Guohua Liu, Yansheng Yan, Hui Yuan, Yuelong Shu, Weizhong Yang, Yu Wang, Fan Wu, Timothy M. Uyeki, and Zijian Feng. Epidemiology of Human Infections with Avian Influenza A(H7N9) Virus in China. *New England Journal of Medicine*, 370(6):520–532, February 2014. ISSN 0028-4793, 1533-4406. doi: 10.1056/NEJMoa1304617.

Qun Li, Xuhua Guan, Peng Wu, Xiaoye Wang, Lei Zhou, Yeqing Tong, Ruiqi Ren, Kathy S.M. Leung, Eric H.Y. Lau, Jessica Y. Wong, Xuesen Xing, Nijuan Xiang, Yang Wu, Chao Li, Qi Chen, Dan Li, Tian Liu, Jing Zhao, Man Liu, Wenxiao Tu, Chuding Chen, Lianmei Jin, Rui Yang, Qi Wang, Suhua Zhou, Rui Wang, Hui Liu, Yinbo Luo, Yuan Liu, Ge Shao, Huan Li, Zhongfa Tao, Yang Yang, Zhiqiang Deng, Boxi Liu, Zhitao Ma, Yanping Zhang, Guoqing Shi, Tommy T.Y. Lam, Joseph T. Wu, George F. Gao, Benjamin J. Cowling, Bo Yang, Gabriel M. Leung, and Zijian Feng. Early Transmission Dynamics in Wuhan, China, of Novel Coronavirus–Infected Pneumonia. *New England Journal of Medicine*, 382(13):1199–1207, March 2020. ISSN 0028-4793, 1533-4406. doi: 10.1056/NEJMoa2001316.

Ting-Hui Lin, Xueyong Zhu, Shengyang Wang, Ding Zhang, Ryan McBride, Wenli Yu, Simeon Babarinde, James C. Paulson, and Ian A. Wilson. A single mutation in bovine influenza H5N1 hemagglutinin switches specificity to human receptors. *Science*, 386(6726):1128–1134, December 2024. ISSN 0036-8075, 1095-9203. doi: 10.1126/science.adt0180.

Natalie M. Linton, Andrei R. Akhmetzhanov, and Hiroshi Nishiura. Correlation between times to SARS-CoV-2 symptom onset and secondary transmission undermines epidemic control efforts. *Epidemics*, 41:100655, December 2022. ISSN 17554365. doi: 10.1016/j.epidem.2022.100655.

Yang Liu, Centre for Mathematical Modelling of Infectious Diseases nCoV Working Group, Sebastian Funk, and Stefan Flasche. The contribution of pre-symptomatic infection to the transmission dynamics of COVID-2019. *Wellcome Open Research*, 5:58, April 2020. ISSN 2398-502X. doi: 10.12688/wellcomeopenres.15788.1.

J. O. Lloyd-Smith, S. J. Schreiber, P. E. Kopp, and W. M. Getz. Superspreadering and the effect of individual variation on disease emergence. *Nature*, 438(7066):355–359, November 2005. ISSN 0028-0836, 1476-4687. doi: 10.1038/nature04153.

Ira M. Longini, Azhar Nizam, Shufu Xu, Kumnuan Ungchusak, Wanna Hanshaoworakul, Derek A. T. Cummings, and M. Elizabeth Halloran. Containing Pandemic Influenza at the Source. *Science*, 309(5737):1083–1087, August 2005. ISSN 0036-8075, 1095-9203. doi: 10.1126/science.1115717.

Martha P Montgomery, Sinead E Morris, Melissa A Rolfs, Wanitchaya Kittikraisak, Aaron M Samuels, Matthew Biggerstaff, William W Davis, Carrie Reed, and Sonja J Olsen. The role of asymptomatic infections in influenza transmission: What do we really know. *The Lancet Infectious Diseases*, 24(6):e394–e404, June 2024. ISSN 14733099. doi: 10.1016/S1473-3099(23)00619-9.

Hiroshi Nishiura and Hisashi Inaba. Estimation of the incubation period of influenza A (H1N1-2009) among imported cases: Addressing censoring using outbreak data at the origin of importation. *Journal of Theoretical Biology*, 272(1):123–130, March 2011. ISSN 1095-8541. doi: 10.1016/j.jtbi.2010.12.017.

Thomas P. Peacock, Louise Moncla, Gytis Dudas, David VanInsberghe, Ksenia Sukhova, James O. Lloyd-Smith, Michael Worobey, Anice C. Lowen, and Martha I. Nelson. The global H5N1 influenza panzootic in mammals. *Nature*, 637(8045):304–313, January 2025. ISSN 0028-0836, 1476-4687. doi: 10.1038/s41586-024-08054-z.

Tim Peto, Dominic Affron, Babak Afrough, Anita Agasu, Mark Ainsworth, Alison Allanson, Katherine Allen, Collette Allen, Lorraine Archer, Natasha Ashbridge, Iman Aurfan, Miriam Avery, Ellena Badenoch, Priya Bagga, Rishab Balaji, Ella Baldwin, Sophie Barraclough, Carol Beane, John Bell, Tracy Benford, Susan Bird, Marina Bishop, Angela Bloss, Richard Body, Rosie Boulton, Abbie Bown, Carla Bratten, Chris Bridgeman, Dominic Britton, Tim Brooks, Margaret Broughton-Smith, Pauline Brown, Beverley Buck, Elaine Butcher, Wendy Byrne, Gloria Calderon, Siobhan Campbell, Olivia Carr, Penny Carter, Daniel Carter, Megan Cathrall, Matthew Catton, Jim Chadwick, David Chapman, Kevin K. Chau, Tanzina Chaudary, Shaolin Chidavaenzi, Samatha Chilcott, Bea Choi, Hannah Claasen, Simon Clark, Richard Clarke, Dawn Clarke, Richard Clayton, Kayleigh Collins, Rima Colston, James Connolly, Eloise Cook, Marie Corcoran, Ben Corley, Laura Costello, Caroline Coulson, Ant Crook, Derrick W. Crook, Silvia D'Arcangelo, Mary-Anne Darby, John Davis, Rosaline De Koning, Pauline Derbyshire, Pam Devall, Mark Dolman, Natalie Draper, Mark Driver, Sarah Dyas, Emily Eaton, Joy Edwards, Ruth Elderfield, Kate Ellis, Graham Ellis, Sue Elwell, Rachel Evans, Becky Evans, Marion Evans, Ranoromanana Evans, David Eyre, Codie Fahey, Vanessa Fenech, Janet Field, Alice Field, Tom Foord, Tom Fowler, Mollie French, Hannah Fuchs, Jasmine Gan, Joseph Gernon, Geeta Ghadiali, Narindar Ghuman, Kerry Gibbons, Gurvinder Gill, Kate Gilmour, Anika Goel, Sally Gordon, Tillie Graham, Alexander Grassam-Rowe, David Green, Anna Gronert, Tegan Gumsley-Read, Claire Hall, Bassam Hallis, Sally Hammond, Peter Hammond, Beth Hanney, Victoria Hardy, Gabriella Harker, Andrew Harris, May Havinden-Williams, Elena Hazell, Joanne Henry, Kim Hicklin, Kelly Hollier, Ben Holloway, Sarah J. Hoosdally, Susan Hopkins, Lucy Hughes, Steve Hurdowar, Sally-Anne Hurford, Joanne Jackman, Harriet

Jackson, Ruth Johns, Susan Johnston, Juliet Jones, Tinashe Kanyowa, Katie Keating-Fedders, Sharon Kempson, Iftikhar Khan, Beinn Khulusi, Thomas Knight, Anuradha Krishna, Patrick Lahert, Zoe Lampshire, Daniel Lasserson, Kirsten Lee, Lennard Y.W. Lee, Arabella Legard, Cristina Leggio, Justin Liu, Teresa Lockett, Christopher Logue, Vanessa Lucas, Sheila F. Lumley, Vindhya Maripuri, Des Markham, Emma Marshall, Philippa C. Matthews, Sarah McKee, Deborah F. McKee, Neil McLeod, Antoinette McNulty, Freddie Mellor, Rachel Michel, Alex Mighiu, Julie Miller, Zarina Mirza, Heena Mistry, Jane Mitchell, Mika Erik Moeser, Sophie Moore, Akhila Muthuswamy, Daniel Myers, Gemma Nanson, Mike Newbury, Scott Nicol, Harry Nuttall, Jewel Jones Nwanaforo, Louise Oliver, Wendy Osbourne, Jake Osbourne, Ashley Otter, Jodie Owen, Sulaksan Panchalingam, Dimitris Papoulidis, Juan Dobaldo Pavon, Arro Peace, Karen Pearson, Liam Peck, Ashley Pegg, Suzannah Pegler, Helen Permain, Prem Perumal, Leon Peto, Tim E.A. Peto, Thanh Pham, Hayleah L. Pickford, Mark Pinkerton, Michelle Platon, Ashley Price, Emily Protheroe, Hellen Purnell, Lottie Rawden, Sara Read, Charles Reynard, Susan Ridge, Tom G. Ritter, James Robinson, Patrick Robinson, Gillian Rodger, Cathy Rowe, Bertie Rowell, Alexandra Rowlands, Sarah Sampson, Kathryn Saunders, Rachel Sayers, Jackie Sears, Richard Sedgewick, Laura Seeney, Amanda Selassie, Lloyd Shail, Jane Shallcross, Lucy Sheppard, Anna Sherkat, Shelha Siddiqui, Alex Sienkiewicz, Lavanya Sinha, Jennifer Smith, Ella Smith, Emma Stanton, Thomas Starkey, Alexander Stawiarski, Amelia Sterry, Joe Stevens, Mark Stockbridge, Nicole Stoesser, Anila Sukumaran, Angela Sweed, Sami Tatar, Hema Thomas, Carly Tibbins, Sian Tiley, Julie Timmins, Cara Tomas-Smith, Oliver Topping, Elena Turek, Toi Neibler, Kate Trigg-Hogarth, Elizabeth Truelove, Chris Turnbull, David Tyrrell, Alison Vaughan, John Vertannes, Richard Vipond, Linda Wagstaff, Joanne Waldron, Philip Walker, Ann Sarah Walker, Mary Walters, Jenny Y Wang, Ellie Watson, Kate Webberley, Kimerbley Webster, Grace Westland, Ian Wickens, Jane Willcocks, Herika Willis, Stephen Wilson, Barbara Wilson, Louise Woodhead, Deborah Wright, Bindhu Xavier, Fiona Yelnoorkar, Lisa Zeidan, and Rangeni Zinyama. COVID-19: Rapid antigen detection for SARS-CoV-2 by lateral flow assay: A national systematic evaluation of sensitivity and specificity for mass-testing. *EClinicalMedicine*, 36:100924, June 2021. ISSN 25895370. doi: 10.1016/j.eclinm.2021.100924.

Timothy W Russell, Joseph T Wu, Sam Clifford, W John Edmunds, Adam J Kucharski, and Mark Jit. Effect of internationally imported cases on internal spread of COVID-19: A mathematical modelling study. *The Lancet Public Health*, 6(1):e12–e20, January 2021. ISSN 24682667. doi: 10.1016/S2468-2667(20)30263-2.

Patrick Saunders-Hastings and Daniel Krewski. Reviewing the History of Pandemic Influenza: Understanding Patterns of Emergence and Transmission. *Pathogens*, 5(4):66, December 2016. ISSN 2076-0817. doi: 10.3390/pathogens5040066.

Mrinank Sharma, Sören Mindermann, Charlie Rogers-Smith, Gavin Leech, Benedict Snodin, Janvi Ahuja, Jonas B. Sandbrink, Joshua Teperowski Monrad, George Altman, Gurpreet Dhaliwal, Lukas Finnveden, Alexander John Norman, Sebastian B. Oehm, Julia Fabienne Sandkühler, Laurence Aitchison, Tomáš Gavenčíak, Thomas Mellan, Jan Kulveit, Leonid Chindelevitch, Seth Flaxman, Yarin Gal, Swapnil Mishra, Samir Bhatt, and Jan Markus Brauner. Understanding the effectiveness of government interventions against the resurgence of COVID-19 in Europe. *Nature Communications*, 12(1): 5820, October 2021. ISSN 2041-1723. doi: 10.1038/s41467-021-26013-4.

W. D. Tanner, D. J. A. Toth, and A. V. Gundlapalli. The pandemic potential of avian influenza A(H7N9) virus: A review. *Epidemiology and Infection*, 143(16):3359–3374, December 2015. ISSN 1469-4409. doi: 10.1017/S0950268815001570.

Jack Ward, Joshua W. Lambert, Timothy W. Russell, James M. Azam, Adam J. Kucharski, Sebastian Funk, Billy J. Quilty, Oswaldo Gressani, Niel Hens, and W. John Edmunds. Estimates of epidemiological parameters for H5N1 influenza in humans: A rapid review. *medRxiv : the preprint server for health sciences*, 2024. doi: 10.1101/2024.12.11.24318702.

Charles Whittaker, Gregory Barnsley, Daniela Olivera Mesa, Daniel J Laydon, Chee Wah Tan, Feng Zhu, Rob Johnson, Patrick Doohan, Gemma Nedjati-Gilani, Peter Winskill, Alexandra B. Hogan, Arminder Deol, Christinah Mukandavire, Katharina Hauck, David Chien Boon Lye, Lin-Fa Wang, Oliver J. Watson, and Azra C Ghani. Quantifying the impact of a broadly protective sarbecovirus vaccine in a future SARS-X pandemic, August 2024.

P. Whittle. The Outcome of a Stochastic Epidemic—A Note on Bailey's Paper. *Biometrika*, 42(1/2):116, June 1955. ISSN 00063444. doi: 10.2307/2333427.

WHO COVID-19 Dashboard. <https://data.who.int/dashboards/covid19/cases>. COVID-19 deaths | WHO COVID-19 dashboard.

W. Xu, L. Lu, B. Shen, J. Li, J. Xu, and S. Jiang. Serological Investigation of Subclinical Influenza A(H7H9) Infection Among Healthcare and Non-Healthcare Workers in Zhejiang Province, China. *Clinical Infectious Diseases*, 57(6):919–921, September 2013. ISSN 1058-4838, 1537-6591. doi: 10.1093/cid/cit396.

Yang Yang, M. Elizabeth Halloran, Jonathan D. Sugimoto, and Ira M. Longini. Detecting human-to-human transmission of avian influenza A (H5N1). *Emerging Infectious Diseases*, 13(9):1348–1353, September 2007. ISSN 1080-6040. doi: 10.3201/eid1309.070111.

Supplementary Material

Supplementary Methods

Pandemic potential influenza subtypes

In this study we evaluate the feasibility of controlling outbreaks of selected influenza subtypes that have previously caused sporadic human-to-human outbreaks with pandemic potential. We include A/H5N1, A/H1N1, and A/H7N9. These have caused outbreaks of various size and severity over the past 100 years. H5N1 has caused small outbreaks (< 10 cases) of human-to-human transmission (Yang et al., 2007; Aditama et al., 2012). H1N1 is now an endemic seasonal influenza with substantial population immunity, but a novel strain, H1N1pdm09, emerged in 2009 and caused a pandemic outbreak (Fraser et al., 2009; Lessler et al., 2009). The first human case with the H7N9 subtype was in 2013, subsequently causing five outbreak waves, but no human cases since 2019 (Li and Chen, 2021). Most cases are of zoonotic origin with recorded animal exposure but there have been some small clusters (2 – 3 cases) of possible human-to-human transmission (Li et al., 2014). For the purposes of this study we assume that there is no preexisting population immunity for these influenza subtypes. This is generally true for H5N1 and H7N9 at present, and for H1N1pdm09 prior to 2009.

Transmission model generation time from incubation period

Here we provide a more detailed description of how the generation time is calculated from the incubation period. The time between an infector being infected and then infecting an infectee (i.e. generation time) is computed using the incubation period (which samples the symptom onset time from the exposure time of each case) and sampling from a skew-normal distribution (Azzalini, 1985). This approach enables simulating transmission dynamics with a correlated structured between each case's incubation period and generation time for sensible delays between exposure, onset of symptoms, and onward transmission (Hellewell et al., 2020; Linton et al., 2022). This allows the proportion presymptomatic transmission to be specified, rather than defining incubation period and generation time distributions, which only indirectly allows assumptions of presymptomatic infectiousness to be derived. This simple formulation is advantageous for novel pathogens and early in outbreaks when the incubation period is estimated but the generation time is estimated with more uncertainty or unknown, and the serial interval cannot be substituted in without introducing bias (Britton and Scalia Tomba, 2019; Lehtinen et al., 2021).

Given the incubation period for each case, the proportion of the infections that occur prior to, or after, the symptom onset of an infector is controlled by the parameterisation of the skew normal distribution (Figure 2C). The symptom onset time is used as the location parameter (ξ) of the distribution, providing the point around which the distribution is dispersed. The scale parameter (ω) is fixed at 2, this parameter (with the shape parameter) defines the variance of the distribution. We select this value as it provides a realistic amount of variance when transforming onset time to exposure time (variance range for scenarios in this study: 1.5 – 3.2). The shape parameter (α) defines the skewness of the distribution, whereby positive values cause right-skewed values distribution around the location ξ , and negative values have the opposite effect (as $\alpha \rightarrow \infty$, the skew-normal converges to a folded-normal distribution). In summary, for a given parameterisation of the skew-normal distribution given the time of symptom onset (ξ) and fixing ω and α we sample the time an infectee is exposed/infected by an infector.

We parameterise the skew-normal with three proportion of presymptomatic transmission scenarios: 1%, 15%, 30%, these correspond to α values of 31.82053, 1.962614, and 0.726558, respectively (Figure 2C).

Modelling non-pharmaceutical interventions

The epidemic simulation model uses a single-type branching process with a negative binomial offspring distribution to simulate the spread of a pathogen through a population (infinite population size, without depletion of susceptibility). Influenza subtypes have shown moderate transmission heterogeneity (Fraser et al., 2009; He et al., 2020; Ward et al., 2024), but evidence is limited and the negative binomial allows flexibility between highly heterogeneous and homogeneous individual-level transmission. The mean of the negative binomial offspring distribution is the basic reproduction number (R), and this distribution allows the model to be parameterised to capture overdispersion of transmission, in other words, some infectors are superspreaders and infect a disproportionate number of individuals (Lloyd-Smith et al., 2005; Kucharski et al., 2020).

There are three categories for individuals in the simulation, with each having their own parameterisation for the negative binomial offspring distribution: 1) *community* (i.e. general population), 2) *isolated*, and 3) *asymptomatic*. Each group have a distinct R and dispersion (k) parameter due to the assumed differences in transmission dynamics between groups.

The NPI implemented in the transmission model is an isolation of symptomatic cases and contact tracing (Figure 1). When a case is symptomatic they are isolated after a delay. The timing of isolation is drawn from the onset-to-isolation distribution. Any infection times that are sampled to occur after the isolated of an infector are removed, because isolation

is assumed completely effective at preventing further transmission, reducing the number of secondary cases if the speed of isolation is quicker than some or all of the secondary infection times. In other words, once a case is isolated at time $t_{isolated}$, the probability of that case infecting anyone at $t > t_{iso}$ is zero. Another way to interpret the model is that R is composed of secondary infections before isolation (R_{pre}) and secondary infections after an assumed isolation time (R_{iso}). Symptomatic individuals that are traced are isolated either when 1) the onset-to-isolation delay after symptom onset, or 2) the infector is isolated. The isolation of the infectee is whatever occurs first of these two events.

Defining outbreak control

Outbreak control, or the extinction or elimination of the pathogen, is a binary classification, which is true if there are no new cases from the 12th week of the outbreak onwards, and false otherwise. This is the same definition as used in Hellewell et al. (2020). The 12 week threshold is somewhat arbitrary but is judged to be long enough that the NPIs can bring the effective reproduction number below one for all transmission to cease. The number of generations in an outbreak lasting 12 weeks will be approximately between 18 generations (H5N1 median incubation period and 0.1% presymptomatic transmission) and 84 (H1N1 median incubation period and 30% presymptomatic transmission), although realisations of the stochastic simulation may be greater or less than these estimates from distribution medians.

The maximum number of cases in each simulation replicate before terminating the simulation and concluding it is uncontrolled was set to 5,000. This number should be larger than the expected cluster size from a subcritical outbreak which is given by $N_i/(1 - R)$, where N_i is the number of initial cases and R is the reproduction number. For example, using the largest initial outbreak size in this study $N_i = 40$, and assuming R is subcritical but very close to unity, $R = 0.99$, gives a possible outbreak size of 4,000 cases. Therefore, our limit that 5,000 cases is an uncontrolled outbreak should not include any outbreaks that will go to extinction eventually but produce transient outbreaks by chance.

For computational efficiency we capped the maximum number of days the simulation could run for to 140 (20 weeks). This is substantially longer than the 12 cutoff evaluating outbreak control so does not influence the results.

Supplementary Results

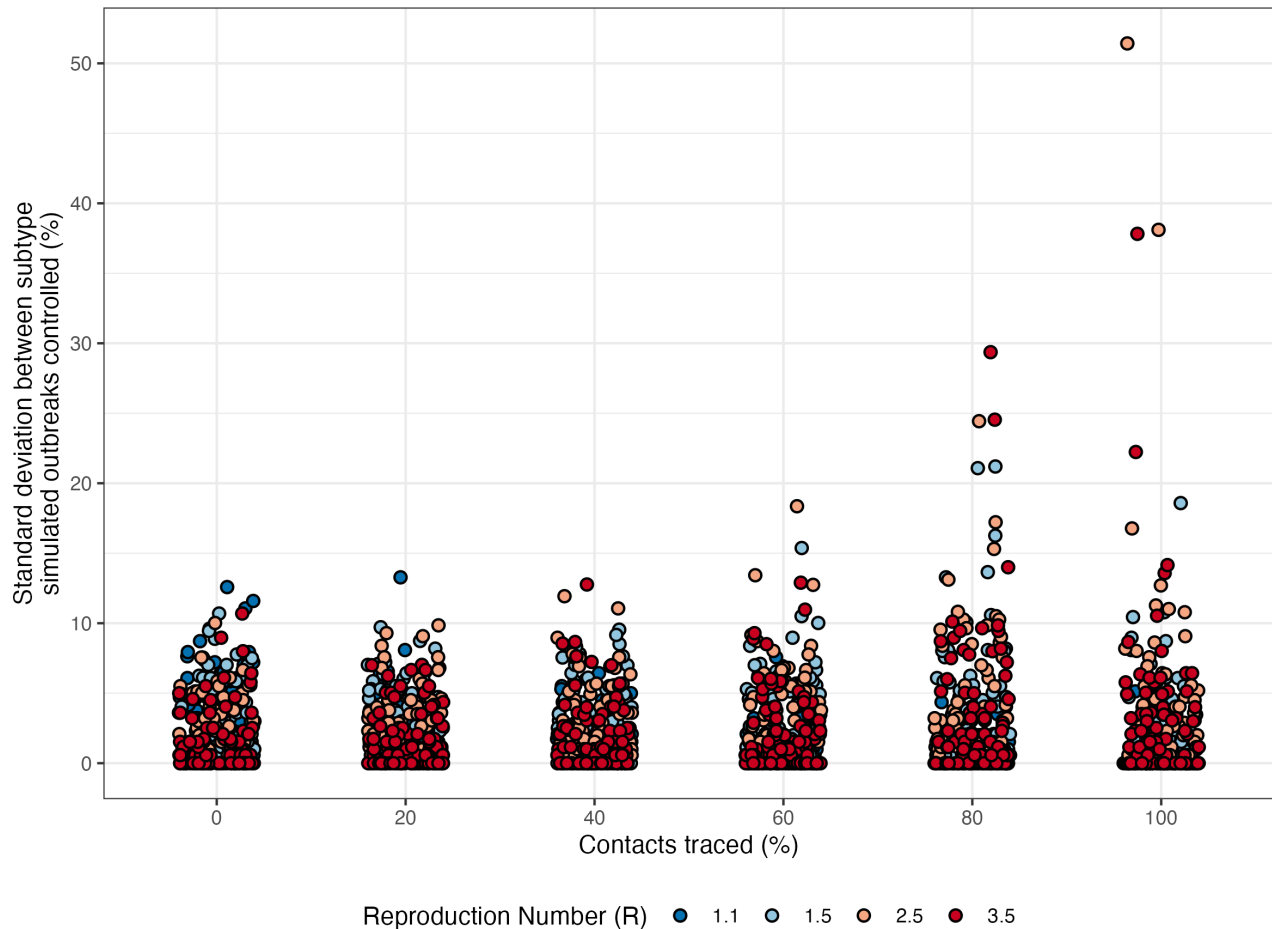


Figure S1: The standard deviation of the percentage of outbreaks controlled between influenza subtypes (H1N1, H5N1, H7N9), across percentages of contacts traced. Points are jittered horizontally reduce overlap.

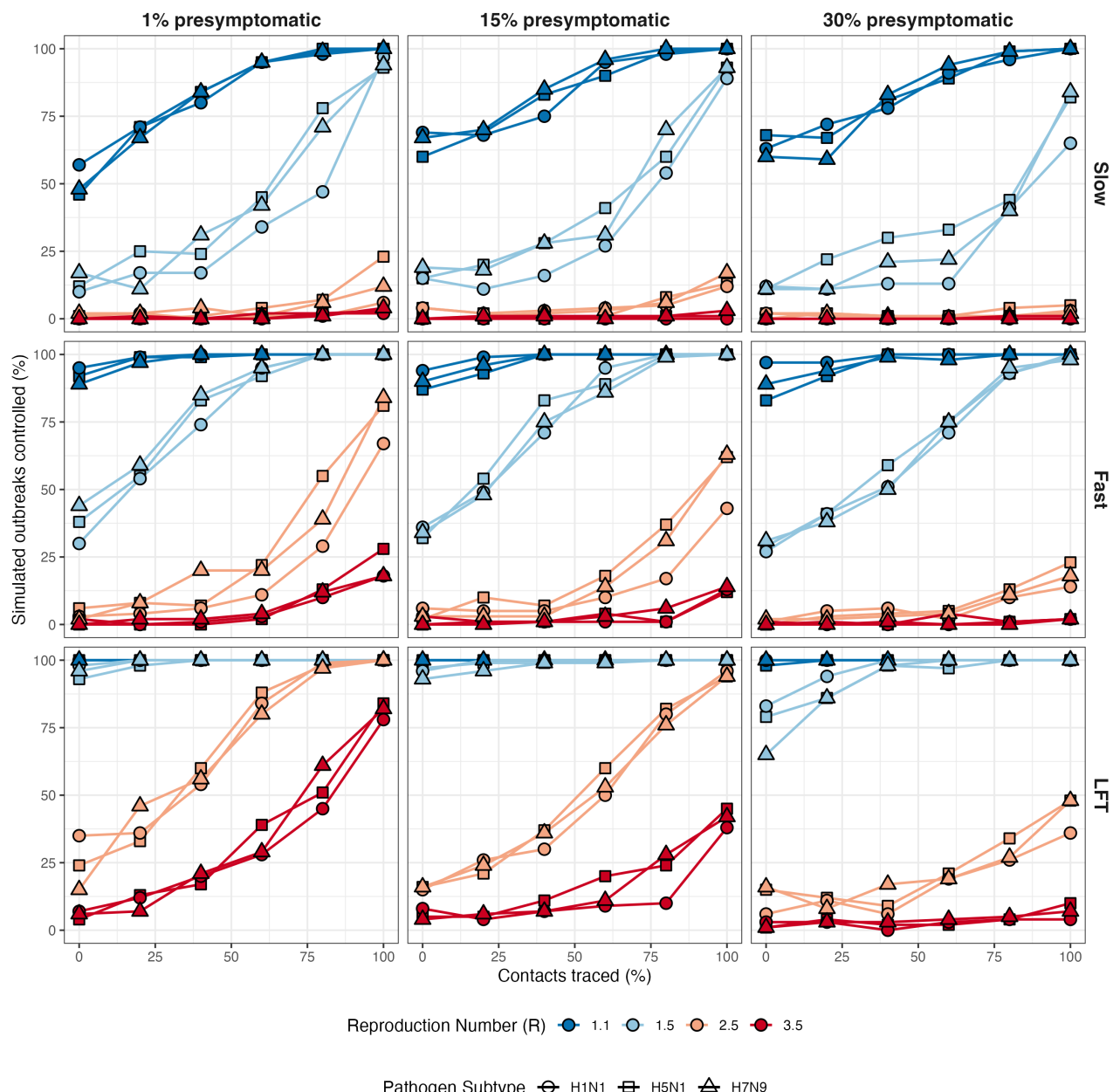


Figure S2: Stub.

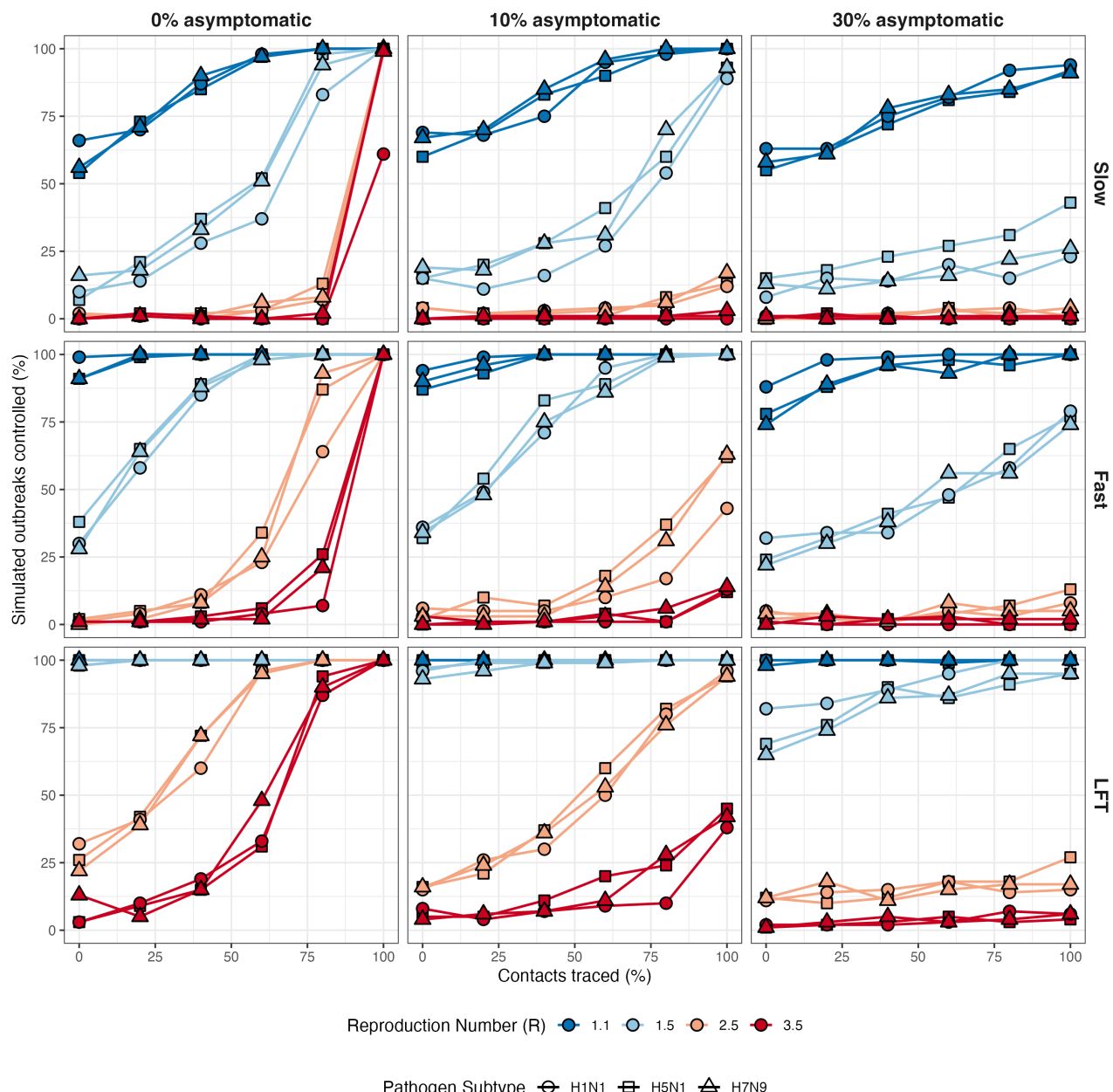


Figure S3: Stub.

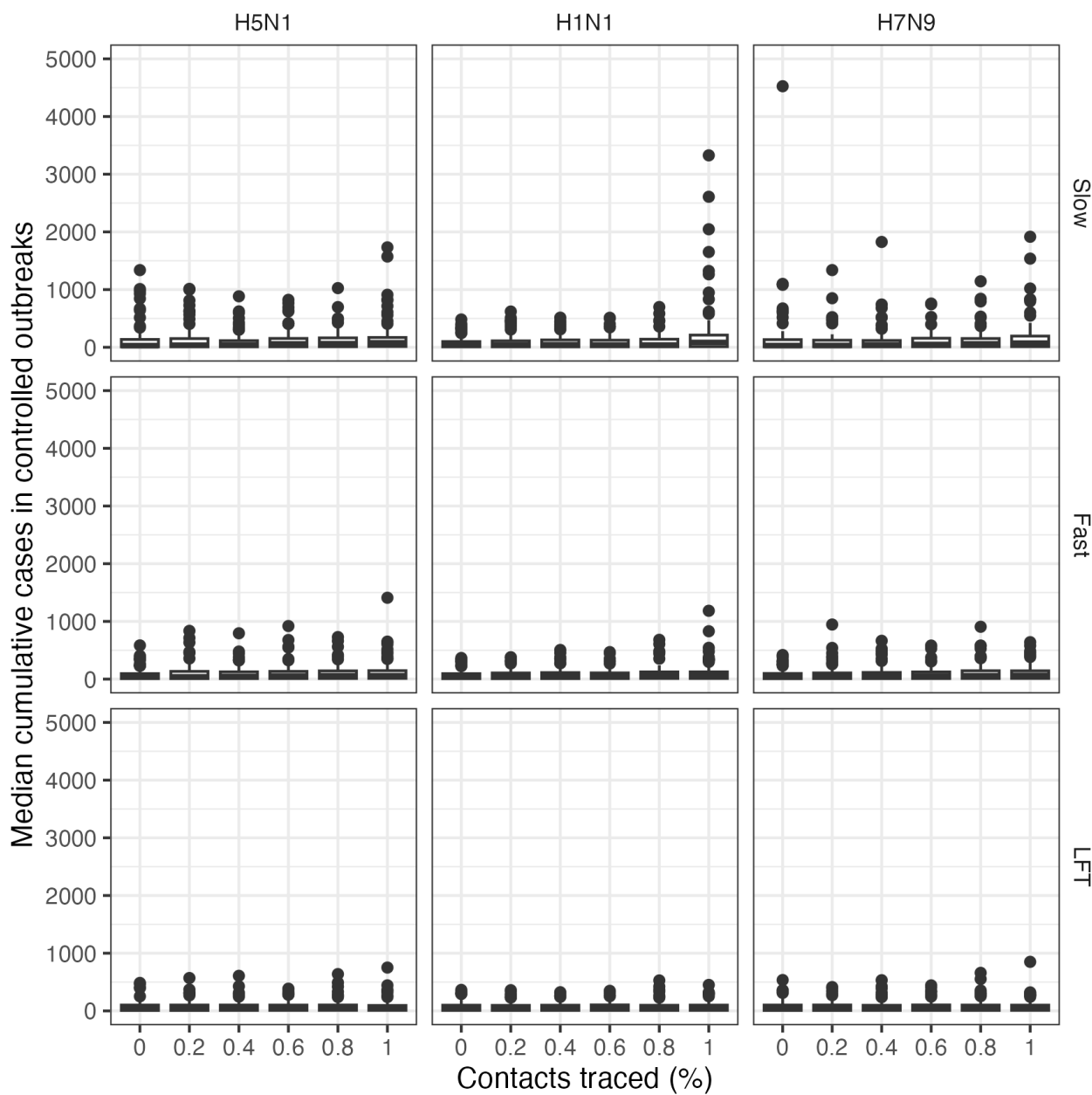


Figure S4: Median...

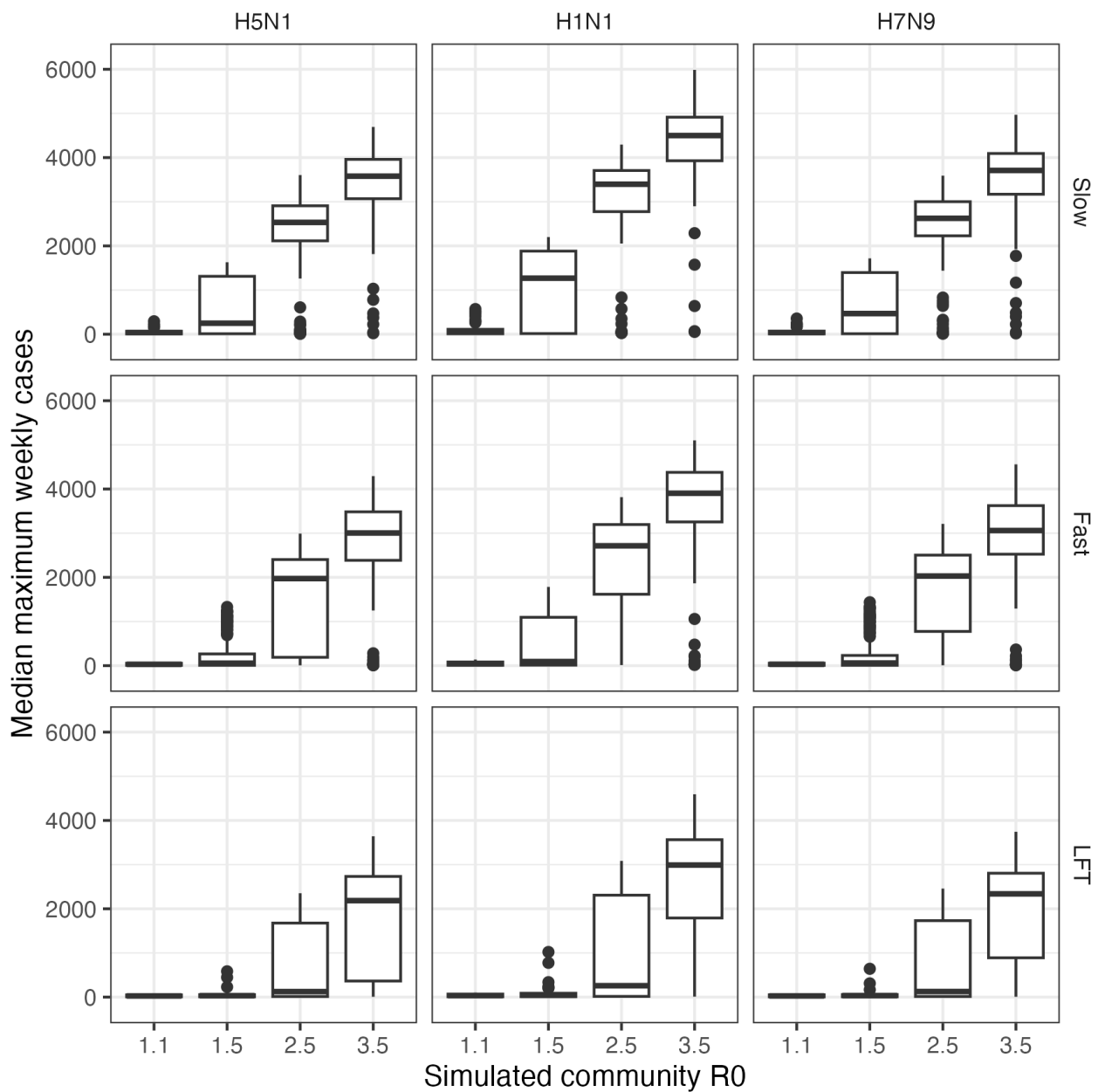


Figure S5: The median maximum number of weekly cases across simulation replicates for different values of community reproduction number (R_0). This is faceted by influenza subtype (A/H5N1, A/H1N1, A/H7N9) and onset-to-isolation response delays (slow COVID-like response, fast SARS-like response and LFT self-testing). The boxplots contain all scenarios (e.g., proportion of asymptomatic cases or number of initial cases) within that reproduction number scenario, the whiskers correspond to the 25th and 75th quartiles. Data outside of $1.5 \times$ the interquartile range are plotted as outlier points.

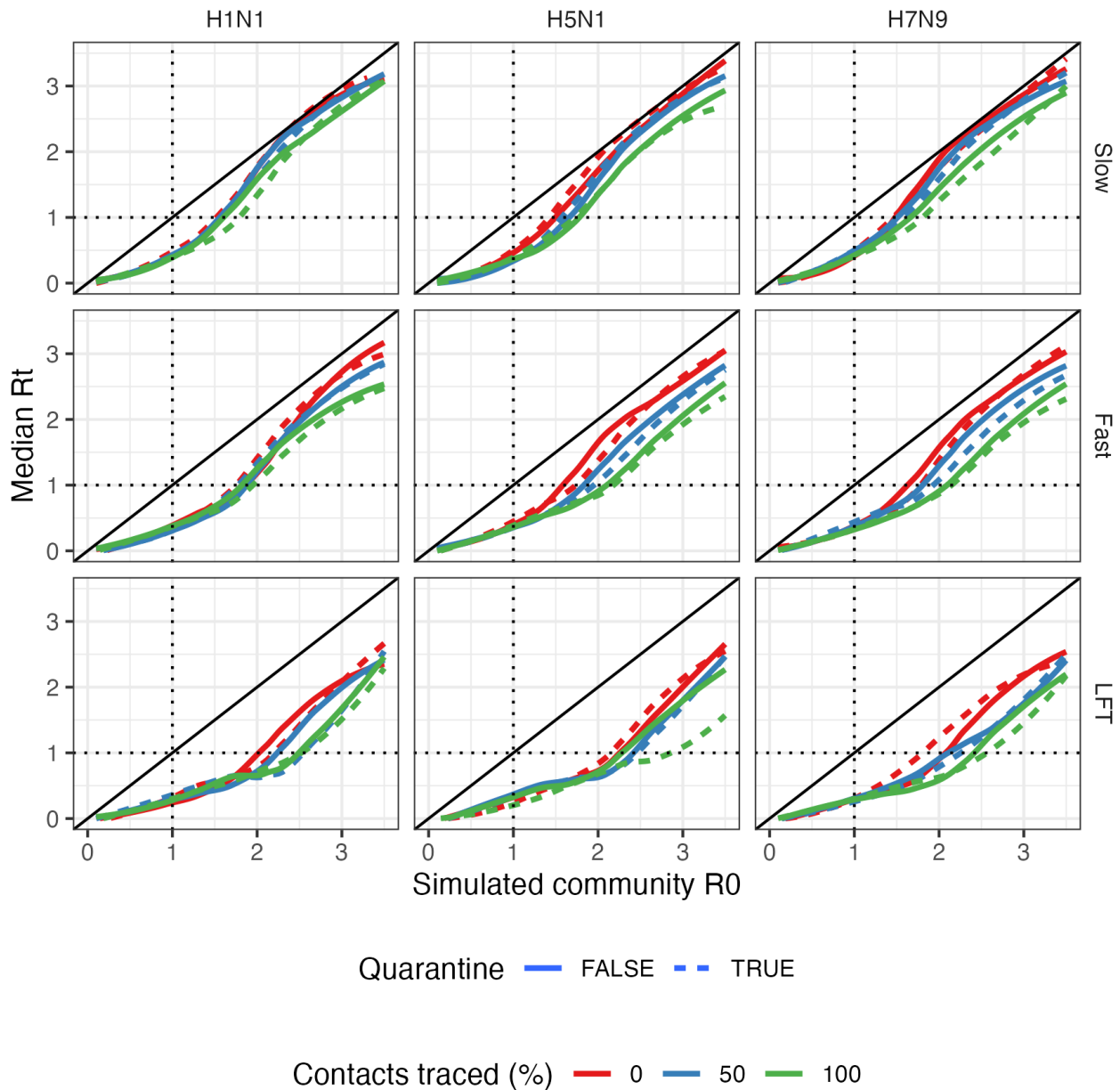


Figure S6: The median effective reproduction number (R_t) across simulation replicates calculated from simulated outbreak data under various influenza subtype and intervention scenarios against the basic reproduction number (R_0) for the general community used to simulate the outbreaks. The R_0 value for isolated cases is zero. The diagonal line shows an equal value for R_t and community R_0 . The dotted lines are where the values of R_t (horizontal) or community R_0 (vertical) equal unity. Values of R_t below the diagonal indicate a reduction in transmission from NPIs compared to uncontrolled community transmission. Isolation of symptomatic cases is active for all scenarios, contact tracing ascertainment is plotted for 0% (no contact tracing), 50% and 100% (all symptomatic contacts of symptomatic cases traced), we run each scenario with quarantine of contacts active (dashed line) and inactive (solid line). This is for a baseline scenario where the proportion of presymptomatic transmission is 1% and the proportion of asymptomatic cases is 0%.